Coordination Chemistry Reviews 255 (2011) 649–663

Contents lists available at ScienceDirect

Coordination Chemistry Reviews

journal homepage: www.elsevier.com/locate/ccr

Review

Moving the frontiers in solution and solid-state bioNMR

Ivano Bertini*, Claudio Luchinat, Giacomo Parigi

Department of Chemistry and Magnetic Resonance Center (CERM), University of Florence, Via Sacconi 6, 50019 Sesto Fiorentino, Italy

Contents

1. Introduction 649
2. Structural and mobility studies in multidomain systems 650
   2.1. Monitoring the conformational heterogeneity in the diamagnetic protein MMP-12 650
   2.2. Monitoring the conformational heterogeneity in calmodulin using paramagnetism-based restraints 652
   2.3. Monitoring the conformational heterogeneity in protein complexes 655
   2.4. Exploiting paramagnetism-based restraints for structural studies in solution 656
3. Exploiting paramagnetic restraints in solid-state structural studies 658
4. ^{13}C direct detection for paramagnetic systems in liquid and solid-state NMR 659
5. Combining solution and solid-state NMR to study large molecules 660
6. Concluding remarks 661
   Acknowledgements 661
   References 661

ARTICLE INFO

Article history:
Received 3 June 2010
Accepted 5 September 2010
Available online 17 September 2010

Dedicated to Harry B. Gray who has been an inspiring model for Ivano Bertini in science and life. The visit of Ivano Bertini to Caltech in 1974 triggered the flourishing of biological inorganic chemistry in Florence. Then a deep friendship developed involving the coauthors of the present article and all the faculty staff at CERM and beyond.

Keywords:
Paramagnetic molecules
Conformational heterogeneity
Solid-state NMR
Pseudocontact shifts
Self-orientation residual dipolar couplings
^{13}C direct detection

ABSTRACT

A major research field in mechanistic systems biology is represented by the development of methods for investigating the structural and dynamic features of systems with multiple interacting components, in order to understand their function. A combination of NMR techniques can be used in such respect, among which the employment of paramagnetic metal ions, ^{13}C direct detection, and solid-state NMR, possibly supported by other techniques like small angle X-ray scattering. Among the results, the information on the conformational heterogeneity experienced by multicomponent systems in solution can be mentioned. The structural and functional characterization of large biological systems, not affordable with standard solution NMR techniques, can be tackled through a synergistic use of solution and MAS solid-state NMR. ^{13}C direct detection NMR spectroscopy is on the other hand advantageous for improving the quality and quantity of observed nuclear signals, for their intrinsically smaller linewidths and larger signal breadth. Details on these approaches are reviewed here.

© 2010 Elsevier B.V. All rights reserved.

1. Introduction

NMR is a well-known powerful tool for the investigation of protein structures and mobility in solution [1–5]. In turn, protein mobility has been shown in several cases to be strongly correlated to function [6–10]. Therefore, numerous efforts have been made in the last years to develop methods able to increase the accuracy and the quantity of information needed to characterize the conformational variability of proteins and protein complexes in solution.

In recent years, solid-state ^{13}C NMR has also emerged as a unique technique for the structural characterization of systems that cannot be easily studied in solution or by X-ray diffraction. ^{13}C direct detection represents an emerging tool also in solution NMR, i.e. for better exploiting paramagnetic systems and

* Corresponding author.
E-mail address: ivanobertini@cerm.unifi.it (I. Bertini).

0010-8545/$ – see front matter © 2010 Elsevier B.V. All rights reserved.
doi:10.1016/j.ccr.2010.09.001

tackling large complexes, which nicely complements solid-state NMR experiments, also thanks to the ease of transferring assignments from the liquid state to solid-state spectra [11]. The combined use of both techniques may provide access to relevant information on systems not affordable using a single technique.

Several NMR techniques have been used to detect mobility in proteins. The presence of fast motions can for instance be indicated by heteronuclear relaxation measurements, or by cross-correlation relaxation rate constants that result from the interference between the $^{1}H–^{15}N$ dipole–dipole coupling and ^{15}N chemical shift anisotropy interactions [2,12]. An order parameter S^2 is obtained without invoking any specific model for internal motion, which measures the magnitude of the angular fluctuation of a chemical bond vector (such as the $N–^{N}H$ bond), and thus reflects the mobility at that site. Recently, relaxation rate measurements of protein protons from very low fields up to high fields have also been proposed [13,14]. In this way the spectral density function of the observed nuclei can be directly accessed, and used to define a collective order parameter, S_C^2. The latter depends on the motional averaging of all kinds of proton-proton interactions, including long-range ones, which are certainly more sensitive to internal motions from the picoseconds to the nanoseconds time ranges than backbone amide protons. Such measurements performed on the protein calmodulin in its calcium-free form indicate that its reorientation time is in agreement with a closed form of the protein, and that the collective order parameter is much smaller than for other well-folded compact proteins, so that a remarkably large side chain mobility must be present [15].

Biochemically significant properties, such as protein local stability and interactions, are often related to motions occurring on a slower time scale, which reflect motions due to chemical exchange or conformational equilibria. Motions in the microsecond to millisecond time scale can be detected through CPMG, $R_{1\rho}$ experiments, or ^{15}N R_2/R_1 values [2,12,16–20]. Residual dipolar couplings (rdc) are sensitive to motions on any time scale faster than milliseconds [21,22]. Due to their large sensitivity to the direction of the vector connecting the two coupled nuclei with respect to a protein common frame, rdc can in fact monitor any change in protein conformation with respect to a structural model. Deviations in the measured rdc values with respect to the values calculated according to the protein model may thus indicate inaccuracy in the latter, so that the rdc can be used for its refinement. On the other hand, deviations still present for more than one set of rdc data after the refinement of the protein structure may reveal the presence of motions. All the above techniques, however, although extremely useful for detecting the presence of mobility within the protein, can hardly provide the ensemble of conformations experienced by the system. Ensemble average approaches, possibly assisted by molecular dynamics calculations, have been more recently introduced to improve the agreement in the fit of motional-averaged NMR data, like rdc, chemical shifts, paramagnetic relaxation enhancements, and to reproduce the values of the heteronuclear relaxation derived S^2 parameters [5,8,23–27].

The presence of a paramagnetic metal ion in the investigated system represents a major source of information for both its structural and dynamic characterization [28–31], particularly useful for proteins with domains experiencing flexibility, such as multidomain proteins, and for protein–protein complexes. Some examples will be discussed where it is shown how the presence of a paramagnetic ion can add precious information for the characterization of the protein structure and of structural equilibria. In the examples selected here, paramagnetic pseudocontact shift (pcs) and residual dipolar coupling (rdc) restraints are obtained through substitution of the diamagnetic metal ion with a paramagnetic ion. In other cases, paramagnetic tags can be attached to the protein under investigation [32–35], so that pcs and rdc become available, provided the tags are rigidly attached [36–40]. Rigidity is achieved by two-point attachment on non mobile residues on the surface of the protein through two disulfide bonds [41,42], by anchoring to the target protein via a disulfide bridge and the N-terminal fusion [43], by a single covalent bond and additional coordination of the paramagnetic ion by an amino acid of the protein [37,44] or by a bulkier metal ion binding cage attached through a single covalent bond [45]. For a recent review on the development and applications of paramagnetic tags for protein NMR studies we refer to the works by Otting et al. [46,47] and by Allen and Imperiali [48].

2. Structural and mobility studies in multidomain systems

2.1. Monitoring the conformational heterogeneity in the diamagnetic protein MMP-12

Multidomain proteins can easily sample a collection of conformations through the presence of flexible linker(s) connecting rigid domains. Matrix Metalloproteinases (MMPs) are extracellular proteins constituted by two rigid domains (except MMP-7), named catalytic domain and hemopexin-like domain, connected by a linker the length of which varies from 14 to 68 residues. A comparison of the available solution and crystal structures of the catalytic domains of different MMPs actually indicate that even within the catalytic domain itself they show a certain degree of disorder in the same loop regions [49]. The presence of such disorder was confirmed in MMP-12 by $^{1}H–^{15}N$ relaxation, $R_{1\rho}$ and CPMG measurements (which show motions on the millisecond to microsecond time scales), by residual dipolar coupling measurements (which encompass the effects of motions on all time scales faster than milliseconds), and by the presence of resonance splitting for several residues in the $^{1}H–^{15}N$ HSQC spectra (which indicates the presence of multiple conformational states with life time of the order or longer than tens of milliseconds) [49].

MMPs are involved in a number of processes including degradation and remodelling of the extracellular matrix [50]. Although the catalytic domain alone has a proteolytic activity, proteolysis of triple helical collagen requires the full length protein [51], so that a model has been proposed with the hemopexin-like domain unwinding the triple helix in such a way that a single peptide strand can be accommodated and cleaved in the active site of the catalytic domain [52,53]. Such a model requires that the hemopexin-like domain is mobile with respect to the catalytic domain.

By comparing the crystal structure of the available full length MMPs, MMP-1, MMP-2 and MMP-12 [54,55], the catalytic domains of the three proteins were found to nicely superimpose, and also the hemopexin-like domains showed the same fold, but the relative orientation of the two domains was completely different. The two domains of MMP-12 actually interact separately with the linker residues, without extensive direct interactions, differently from the MMP-1 and MMP-2 cases [55]. Such conformational variability and the lack of direct domains interactions, together with the fact that when calculating the crystal structure of MMP-12, the electron density was of generally good quality throughout the whole molecule (with crystals diffracting to 3.0 Å resolution) except for the residues in the middle of the linker region, suggested the possibility that in solution the two domains are relatively free to move thanks to the flexible linker. Solution NMR measurements actually confirmed this model [55]. Such experiments were performed on the NNGH-inhibited, cadmium(II)-substituted Phe171Asp/Glu219Ala double mutant of full length MMP-12, in order to prevent self-proteolysis; analysis of the $^{1}H–^{15}N$ HSQC spectra anyway revealed that mutations and substitution of the catalytic zinc(II) ion did not cause relevant structural alterations. The lack of interdomain NOEs and the fact that the peaks of the catalytic and hemopexin-like domain

residues in the $^{1}H–^{15}N$ HSQC spectrum of the full length protein were about in the same position observed in the spectra for the isolated domains indicate that the two domains do not really interact in solution.

Relaxation rate experiments were performed on the full length protein as well as on the isolated catalytic and hemopexin-like domain. Whereas both the longitudinal R_1 and transverse R_2 relaxation rates measured for the amide protons in the two isolated domains agree with the values calculated from the atomic coordinates of the domain structures by using the program HYDRONMR [56], which assumes a rigid-body hydrodynamics, the experimental R_1 values are sizably larger and the experimental R_2 sizably smaller than the calculated values in the case of the full length protein (Fig. 1A). The relaxation rate values measured for the full length protein are indeed intermediate between the isolated domains and the rigid full length crystal structure. On the other hand the ^{15}N NOE values for the full length MMP-12 show that the single domains behave as rigid structures, in agreement with the invariance of the $^{1}H–^{15}N$ HSQC spectra and the NOESY patterns, and that some linker residues are affected by conformational variability. This proves that the interdomain linker must be flexible, thus allowing extensive reciprocal reorientation of the two protein domains on a time scale faster than the reorientational time of the whole molecule.

Further evidence of the conformational heterogeneity of the protein due to flexibility of the interdomain linker was obtained through the measurement of the residual dipolar couplings (rdc) arising in the presence of an external orienting medium. The rdc data were first found in disagreement with the crystal structure, as no good fit by any orienting tensor could be obtained. The same rdc data, when considered separately for the two domains, could instead be satisfactorily fitted to the corresponding domain structures, but the orienting tensors calculated for the two domains did not agree with one another (Fig. 1B). This proves that the external medium orients the two domains independently as a result of the lack of a rigid structure for the whole molecule.

In order to gain information on the conformational ensemble corresponding to the full length MMP-12, Small Angle X-ray Scattering (SAXS) measurements were performed. SAXS intensities in fact depend on the overall shape of the electronic density of the protein [57,58] and, despite not being a probe for mobility, they can provide information on the preferred relative positions of the two protein domains. Neither individual protein conformations nor averaging over ensembles of conformations generated by random movements of the linker provided a calculated scattering curve in good agreement with the measured full length MMP-12 SAXS curve. Ensembles of conformations were then searched using a genetic algorithm in order to obtain a best fit of the experimental data (Fig. 1C). Such ensembles, although not representing unique solutions, provide information on the region of space that the protein preferentially occupies, i.e. on the preferred conformations of the system. They indicate that the protein spends about half of the time in a conformation as compact as the crystal structure (but with different relative interdomain orientation), and the rest in a variety of more extended conformations. The distribution of the radius of gyration corresponding to the different conformational ensembles in fact displays a relatively sharp peak around 28–29 Å, correspond-

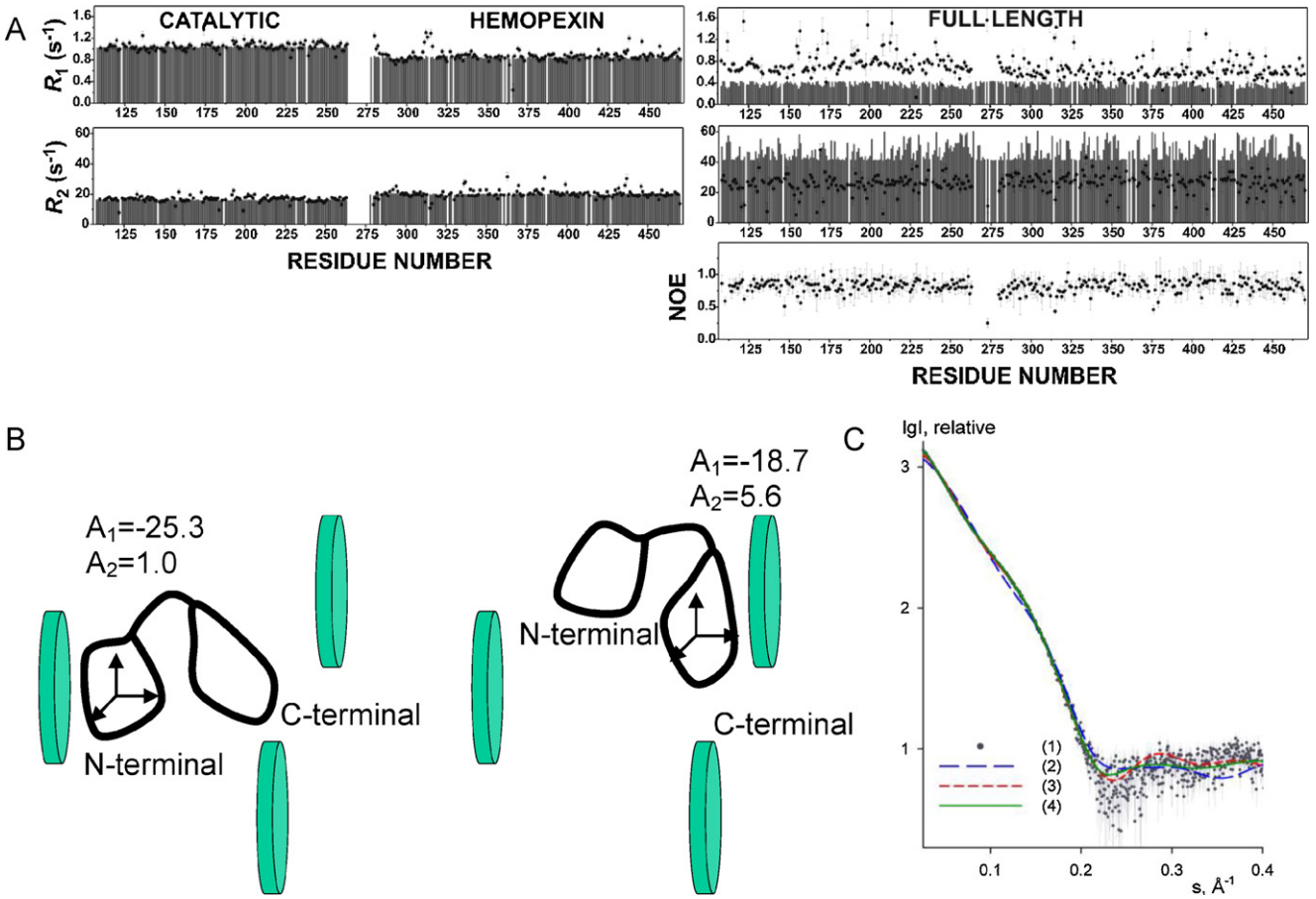

Fig. 1. Mobility studies performed on MMP-12: (A) Calculated (bars) and experimental (points) ^{15}N R_1, R_2 and NOE for the isolated domains and for the full-length protein. The agreement in the R_1 and R_2 values is good for the isolated domains but unsatisfactory for the whole protein. (B) Best fit orientation tensor values for the rdc of the two MMP-12 domains in the presence of an external orienting medium. (C) Experimental (points) and computed (lines) SAXS profiles using crystallographic models (blue and red lines) or best-fit ensembles (green line).

ing to a distance between the two domains similar to that of the crystal structure, but also span the whole range from 30 to 50 Å. Therefore, although the protein conformation observed in the crystal state can be significantly present also in solution, the protein must experience a significant conformational flexibility so that it can sample more extended states. Similar results were obtained also for the MMP-1 protein [59,60], suggesting that this type of conformational freedom is a general property of all MMPs.

2.2. Monitoring the conformational heterogeneity in calmodulin using paramagnetism-based restraints

Calmodulin (CaM), another multidomain protein well known to exhibit interdomain mobility [61–63] is composed of two domains connected by a central linker. Each of the two domains is constituted by two calcium binding EF-hand motifs, and therefore CaM is able to bind up to four calcium ions [64–66]. Calcium binding causes rearrangements in the EF-hand motifs, exposing large hydrophobic clefts on the surface, buried in the calcium-free state, which are responsible for binding to target proteins [66,67]. Inspection of the available protein structures indicates that the helices in each EF-hand move from an almost antiparallel arrangement in the apo form (closed state) to an almost orthogonal arrangement in the calcium-bound form (open state) [62,63,68]. Calcium(II) binding favours CaM-target enzyme binding due to the exposed hydrophobic cores which are surrounded by negatively charged residues. This situation favours the interaction with hydrophobic and positively charged (amphipatic) target peptides. Therefore, the two domains reorient and get closer to one another by clamping the target peptide.

This binding mechanism requires that the two domains of CaM have a certain degree of freedom. The flexible nature of both the inter-domain linker region and of the residues in the hydrophobic cores (Met side chains in particular) would thus provide CaM with the ability to accommodate a variety of targets [69–72]. Furthermore, comparison of the many available structures showed that the target wrap-around binding mode is not the unique binding mode of CaM, as a result of some flexibility within each CaM domain and variability in their relative positioning for adapting to different targets [73].

The mobility of the inter-domain linker was first detected through amide relaxation rate measurements, and in particular by the small NOE values, observed for this protein [61,62], indicating a very high degree of mobility of residues 78–81 and pointing to the presence of extensive motions with a time scale of nanoseconds [62,74]. The sizable flexibility of these interdomain linker residues ensures that the two domains of the protein may freely reorient almost independently of one another [61]. However, these data could hardly provide information on the conformational heterogeneity of the protein. In fact, the ^{15}N R_1 and R_2 values for residues in secondary structure elements were only modestly different from what expected for a rigid structure [62,63] of a well-folded protein. If a motion in a cone is used to visualize the motion related to the relaxation-derived order parameter, the N- and C-terminal domains are expected to wobble independently in cones with a semi-angle of about 27° [62]. Molecular dynamics simulations confirmed the flexibility of the linker [75,76], indicating that CaM can also sample bent and relatively compact conformations.

The first solid-state structure of CaM [77] showed that the last helix of the N-terminal domain, the first helix of the C-terminal domain and the interdomain linker constitute a long-continuous helix. Such conformation was soon recognized to be inconsistent with NMR data. Remarkably, a crystal structure was also obtained later in which the long-interdomain linker is bent and the two domains are in contact with one another [78,79]. It is therefore apparent that, in the case of CaM, the X-ray structures provide different snapshots of the large range of very different conformations that the protein is able to sample in solution. Information on the relative position of the two domains was obtained through the use of paramagnetism-based restraints, i.e. pseudocontact shifts (pcs) and residual dipolar couplings (rdc) [80]. A paramagnetic ion was first bound to the protein by selective substitution of lanthanide ions such as terbium(III), thulium(III) or dysprosium(III) at the second binding site of CaM, with calcium(II) ions binding at the other three sites. Selectivity was achieved by a N60D mutation at the second metal binding loop [81]. In this way pcs and rdc restraints became available.

The pcs of the amide protons of the N-terminal domain of CaM were fit to the CaM solution structure [66] using Eq. (1),

$$\Delta\delta^{pcs} = \frac{1}{12\pi r^3}\left[\Delta\chi_{ax}(3\ \cos^2\theta - 1) + \frac{3}{2}\Delta\chi_{rh}\ \sin^2\theta\ \cos 2\phi\right] \quad (1)$$

where r is the distance between each observed nucleus and the metal ion, θ and ϕ denote the spherical coordinates of the nucleus in the frame of the metal magnetic susceptibility tensor, and $\Delta\chi_{ax}$ and $\Delta\chi_{rh}$ are the axial and rhombic anisotropy parameters of the magnetic susceptibility tensor of the metal. Pcs values depend only on the position of the nucleus with respect to both the metal ion and the paramagnetic susceptibility tensor, besides the values of the anisotropies of the latter. The resulting fit provided the magnetic susceptibility anisotropy tensor of the corresponding lanthanide.

In the presence of motion of the observed nuclei with respect to the metal magnetic susceptibility tensor frame, pcs values are averaged according to the experienced nuclear positions [80,82] and cannot be fit through Eq. (1) using any single protein structure. Motions in the coordination sphere of the paramagnetic ion may also cause modulation of the paramagnetic susceptibility tensor which determines pseudocontact shift modulations. The latter can give rise to line broadening, and the chemical shift difference between the different states can be accessed through relaxation dispersion experiments [42,82,83].

Once the paramagnetic ion is attached to the N-terminal domain, it causes partial alignment of the latter in a magnetic field due to the anisotropy of the paramagnetic susceptibility tensor [84,85]. The C-terminal domain may also experience some partial orientation induced by the structural relationship between the two domains. Therefore, the rdc measured on the nuclei of the C-terminal domain provide information on its relative orientation with respect to the N-terminal domain and, in the presence of interdomain mobility, on the averaging resulting from the individual protein conformations within the sampled ensemble. On the other hand, rdc arising from external orienting media cannot provide the same information because the flexibility of the linker would largely allow the individual domains to be oriented by the external media separately, and in this way the "preferred" conformations sampled in the anisotropic solution would be difficult to recover.

Rdc do not depend on distance (see Eq. (2) below), and therefore the spreading of their values should be approximately the same in both the N- and C-terminal domains, if there were no relative motion between the two (Fig. 2). Indeed, in free CaM, due to the very large interdomain motions, the rdc spreading in the C-terminal domain was only about 5–10% that of the N-terminal domain [80]. By defining a generalized order parameter, S, as the ratio between the spreading of the rdc values in the two domains, a value of about 0.1 is obtained, which would yield an S^2 value of the order of 0.01. This value is much smaller than the value of 0.7 calculated from relaxation rate measurements [62], and is due to the fact that rdc monitor the presence of motions occurring over a much larger range of time scales. Despite the fact that the reduction in the spreading of the rdc values measured for the C-terminal domain with respect to the N-terminal domain is quite large, the rdc spreading for the C-terminal domain is not as small as calculated by

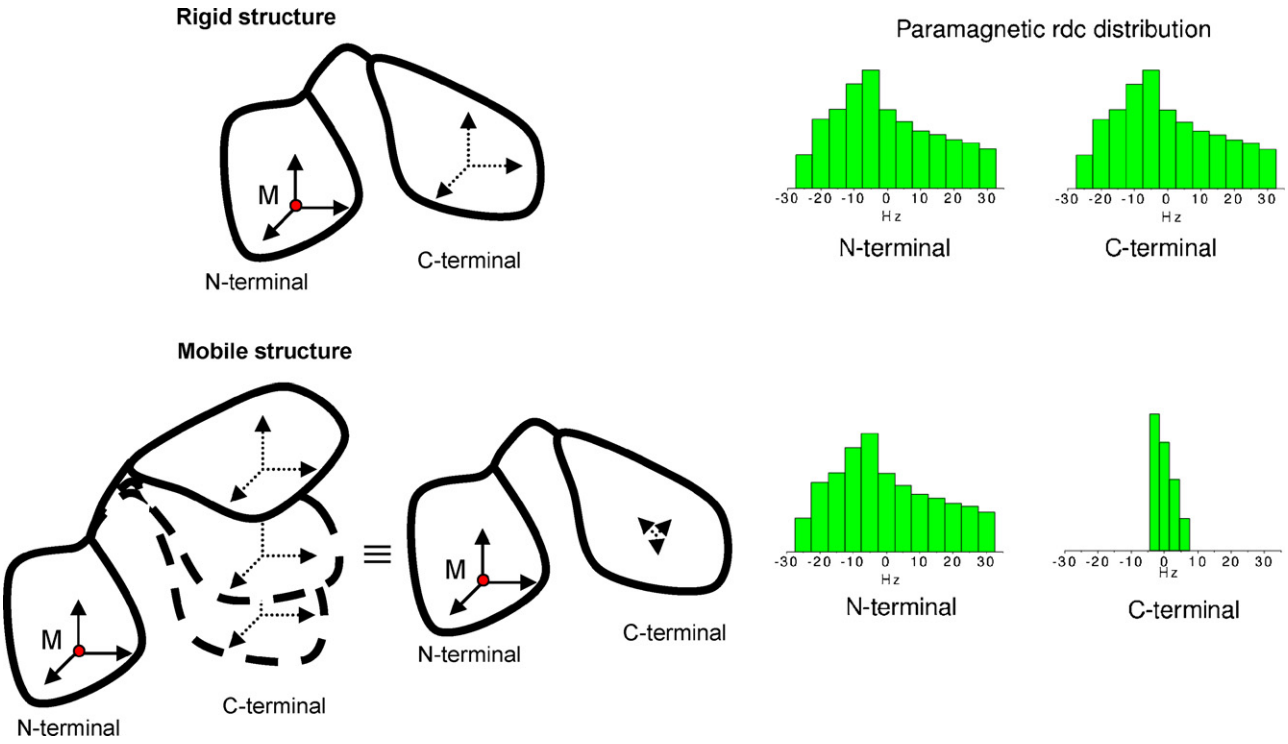

Fig. 2. Distribution of the self-orientation rdc observed for the different domains of a protein with a paramagnetic metal ion in one domain, in the case of a rigid structure or of a structure with a flexible interdomain linker. The rdc of the nuclear pairs in the domain without the metal are determined by the magnitude and orientation of the magnetic susceptibility anisotropy tensor. In the presence of interdomain mobility, the orientation of such tensor changes with respect to the orientation of the domain; the rdc data can still be reproduced by a tensor with a different orientation and with reduced magnitude with respect to the real magnetic susceptibility anisotropy tensor of the metal.

assuming that all sterically allowed conformations are equally populated. Therefore, not all possible protein conformations are equally sampled [80], and the experimental values can be used to extract information on the experienced ensemble of conformations.

Rdc depend on the same magnetic anisotropy tensor present in Eq. (1) [86], according to Eq. (2),

$$\text{rdc}\ \ (\text{Hz}) = -\frac{1}{4\pi}\frac{{B_0}^2}{15kT}\frac{\gamma_N\gamma_H\hbar}{2\pi r_{HN}^3} \times \left[\Delta\tilde{\chi}_{ax}(3\ \cos^2\Theta - 1) + \frac{3}{2}\Delta\tilde{\chi}_{rh}\ \sin^2\Theta\cos 2\Phi\right] \quad (2)$$

where r_{HN} is the distance between the two coupled nuclei (N and ^{N}H for instance) and the spherical angles Θ and Φ are those defining the orientation of the vector connecting the coupled nuclei in the frame of the magnetic susceptibility tensor. Analogously to pcs, $\Delta\tilde{\chi}_{ax}$ and $\Delta\tilde{\chi}_{rh}$ are the axial and rhombic anisotropy parameters of the magnetic susceptibility tensor of the metal. Other symbols have the usual meaning. As already anticipated, rdc values are not related at all to the position of the coupled nuclei with respect to both the metal ion and the magnetic susceptibility tensor, but they depend only on the orientation of the vector connecting the coupled nuclei in the reference frame of the magnetic susceptibility tensor axes [22,84,87,88].

In the free CaM case, we have seen that the experimental rdc values measured for the C-terminal domain are actually much smaller than those calculated using Eq. (2) and the $\Delta\chi_{ax}$ and $\Delta\chi_{rh}$ values obtained from Eq. (1). Correspondingly, the fit of the experimental rdc to Eq. (2) using the CaM solution structure [66] provided axial and rhombic anisotropy values $\Delta\tilde{\chi}_{ax}$ and $\Delta\tilde{\chi}_{rh}$ much smaller than the corresponding values obtained from the tensors derived from the pcs of the N-terminal domain, as a consequence of the presence of a sizable motional averaging (Fig. 2). The agreement of many rdc of the C-terminal domain with a unique tensor for each metal indicated that the whole domain moves essentially rigidly with respect to the N-terminal domain.

The magnetic susceptibility anisotropy tensors obtained from N-terminal domain pcs and the mean tensors obtained from C-terminal domain rdc were then used to calculate the maximum allowed probability MAP(R) that any orientation of the C-terminal domain of CaM has with respect to the N-terminal domain orientation. This MAP(R) represents the maximum weight that the corresponding orientation can have in any conformational ensemble (Fig. 3A). The MAP(R) values can be calculated for all orientations using a geometrical algorithm described in Longinetti et al. [89].

Crucial in this context is the availability of several sets of rdc, related to different magnetic susceptibility tensors resulting from the substitution of several metal ions in the protein. In fact, since rdc are independent of reflections of the axes of the magnetic tensor, quite similar MAP(R) values are calculated for any given orientation as well as for other three symmetric orientations, or *ghost* orientations, if only data referred to two different metal ions are used. In this way the correct relative orientation between the two domains cannot be clearly discriminated from the ghost orientations [89]. In principle, three different metal ions with significantly different magnetic susceptibility anisotropy tensors and good quality rdc values are however enough to eliminate the ghost orientations.

The most representative orientations with largest MAP(R) values were then used as starting points to obtain the conformations, defined by orientation plus translation, with the largest maximum allowed probability, MAP [90]. Therefore, pcs of the C-terminal domains are introduced in the analysis, providing information on the relative position of the protein domain with respect to the metal tensor position. Pcs are also precious to discard ghost orientations still consistent with the rdc data, because they may be inconsistent with the restraint imposed by the length of the interdomain linker.

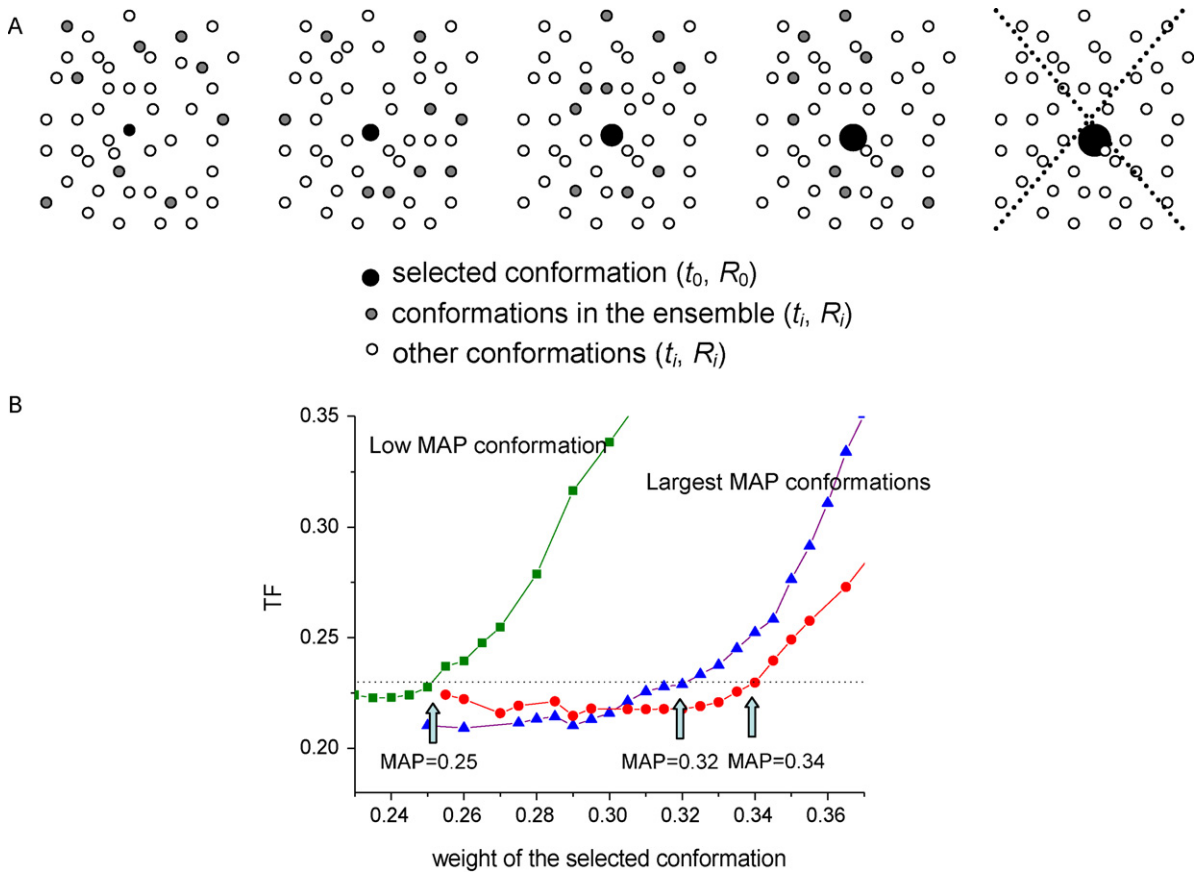

Fig. 3. (A) Experimental averaged data can be reproduced using different ensembles of conformations. The MAP of one selected conformation (solid black sphere) is defined as the maximum weight that such conformation can have and still be part of an ensemble in agreement with the data. In the picture the radius of the selected conformation is proportional to its weight, the gray spheres represent the other conformations present in the ensemble and the open spheres the conformations not present in the solution. When the weight of the selected conformation is larger than its MAP value, no ensemble of conformations is found to reproduce the data. (B) The MAP value for each selected conformation is found as the maximum weight providing a Target Function which is at most 10% higher than the lowest value (dotted line).

Experimentally available pcs, differently from rdc, cannot be calculated from an average tensor, as a consequence of the fact that the distance of the nuclei from the metal ion, from which the pcs values depend, changes due to the interdomain mobility. Largest MAP conformations were thus calculated [90] using an iterative simulated annealing minimization starting from selected orientations (R_0), initially chosen according to the MAP(R) results, complemented by other N conformations, with weight (w_i), position (t_i), and orientation (R_i) obtained in order to minimize the target function

$$TF(w_0) = \min_{t_0,(w_i,t_i,R_i)} \sum_j \left| \tilde{\delta}_j - \left(w_0 \delta_j(t_0, R_0) + \sum_{i=1}^{N} w_i \delta_j(t_i, R_i) \right) \right|^2 \quad (3)$$

where $\tilde{\delta}_j$ are the experimental pcs/rdc values, $\delta_j(t_0, R_0)$ are the pcs/rdc values calculated for the selected orientation R_0, with the translation vector t_0 defining the position of the corresponding conformation, w_0 is the corresponding weight, and $\delta_j(t_i, R_i)$ are the pcs/rdc values calculated for the other $i = 1, \ldots, N$ conformations. Such a function represents the minimal error on the reconstructed data when the domain is constrained to stay in the conformation defined by the orientation R_0 and the translation t_0 for a fraction w_0 of the time whatever other conformations are in the ensemble. The MAP value of this conformation was then defined as the largest w_0 value such that $TF(w_0) = \varepsilon$, where ε is the threshold fixed for the error, set to a value that is 10% larger than the absolute minimum of the TF, as shown in Fig. 3B.

The minimization procedure which is performed may recall the ensemble average approaches which are also used to obtain families of conformations in agreement with averaged experimental restraints. Ensemble average approaches have been successfully used to recover the extent of the conformational variability within the conformational space using NMR data [5,8,25,80], SAS data [91], or both [92–94]. However, the MAP approach focuses on one particular structure within each ensemble, which is the one with as large as possible a weighting factor, and no reliability is granted to the other structures of the ensemble. In this way it is possible to find the maximum weight that a single conformation can have within any possible ensemble of conformations to retain agreement with the experimental data. Of course this does not mean that such conformation really has such weight, but only that such weight is an upper limit. Several simulations performed by generating averaged pcs and rdc data from ensembles of conformations with, e.g. Gaussian distributions around one or two centers have indicated that in most cases the conformations with largest MAP reflect those actually close to the centers of the Gaussian distributions.

In the case of two (or more) rigid domains tethered by flexible linkers, this approach has been preferred with respect to ensemble average approaches because it can be shown that in the presence of averaged tensors sizably smaller than the fixed frame tensor, the averaged rdc data can agree with any conformation if the latter is counterbalanced by a proper set of other conformations, so that none of them can be taken as representative of the conformations really sampled by the protein. If, for instance, rdc data relative to only one metal ion are provided, it is always possible to find

an ensemble in agreement with the averaged data which includes three conformations one of which selected in a completely arbitrary way. If more sets of data relative to additional metal ions are considered, the number of conformations to be added together with the arbitrary conformation increases, but it is still possible to obtain an ensemble which comprises such conformation that is in agreement with the data. In conclusion, there is no uniqueness in the recovered ensemble, and therefore no reliability can be given to the conformations composing the ensemble. In other cases, when the averaged tensors are not much smaller than the fixed frame tensor, i.e. when mobility is small, the degeneracy of the different ensembles of conformations is reduced because only those conformations extending on a well defined, restricted conformational space can be included in ensembles of few tens of equally weighted members. In fact, the weight of the conformations outside this space, that can still be included arbitrarily in the ensemble, must be much smaller than that of the other conformations within this space, so that the latter can be identified.

The conformations of free CaM that have the largest MAP, as obtained from the conformational averaged pcs and rdc values from three lanthanide ions measured on the C-terminal domain, can be clustered in four families [90], reported in Fig. 4A. The MAP values for such conformations are all around 0.36. In all of them the first helix of the C-terminal domain forms quite large angles with the last helix of the N-terminal domain. Similar conformations are calculated by changing one or both the dihedral angles of residues 79 and 80 in the extended crystal structure from the values of the alpha helix region to typical values of the beta sheet region of the Ramachandran plot. However, the actual weight of such conformations can be smaller than their MAP value, and it is likely much smaller for some of them since they must be complemented by a variety of other conformations with smaller weight.

The MAP approach can be conveniently extended by including into the list of the averaged experimental restraints (besides the paramagnetic pcs and rdc restraints) other observables equally averaged over all the conformations experienced by the system in its motion on any time scale faster than milliseconds. In this way, complementary information can be added to better characterize each conformation with a MAP value and restrict the set of conformations with the largest MAP values. In fact, since the problem of recovering the protein conformational ensemble from the averaged data has not a unique solution, collecting several kinds of restraints differently sensitive to averaged parameters may largely help to better discriminate the different conformations according to their MAP. SAXS restraints were actually highly complementary to NMR data, and were thus included in the calculations of the MAP values [95]. The simultaneous fit of the SAXS intensity profile for calcium CaM and of pcs and rdc data collected on its lanthanide derivatives was actually useful in the refinement and selection of the conformations with largest MAP.

Recently, it was shown that, besides providing the conformations with largest MAP, it is computationally possible through distributed grid computing to calculate the MAP value, also called maximum occurrence (MO), of any conformer sterically allowed, in agreement with the available experimental data. In this way, the whole conformational space can be extensively sampled and scored by its MO values. Therefore, it becomes possible to monitor the extent and the shape of the regions with largest MO, as well as to retrieve the regions which cannot be significantly sampled by the system [95]. Calculations performed for the free CaM are shown in Fig. 4B, where the C-terminal domain of the protein is substituted by a tensor centered in the center of mass of the domain, oriented depending on the relative orientation of the two domains, and color-coded with respect to the MO of the corresponding conformation. It was found in this way that the "closed" and "fully extended" conformations trapped in the crystalline forms of CaM have MO of only 5 and 15%, respectively.

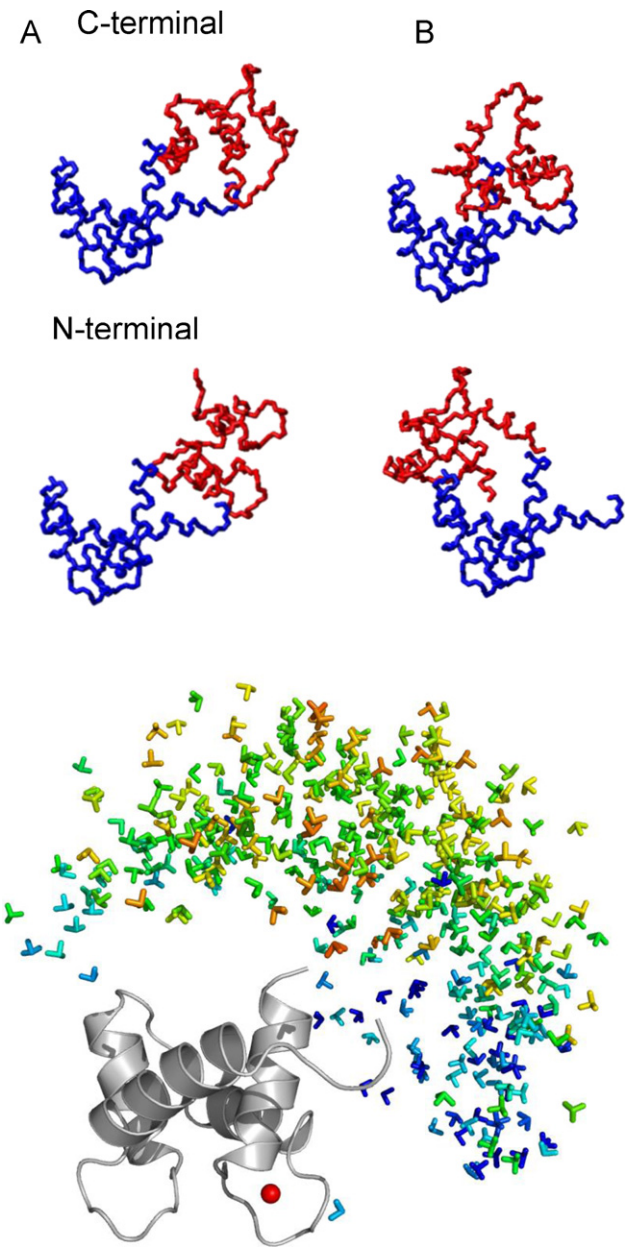

Fig. 4. (A) Conformations with largest MAP of free CaM obtained using pcs and self-orientation rdc. (B) Arbitrary orientation tensors centered in the center of mass of the C-terminal domain of CaM, color-coded with respect to the MO of the corresponding conformation from blue (lower than 5%) to red (greater than 40%) for hundreds of randomly generated structures.

The present data, together with the MMP-1 case previously discussed, represent significant examples of the synergy between NMR and SAXS/SANS techniques.

2.3. Monitoring the conformational heterogeneity in protein complexes

The conformations with largest MAP were determined for the calcium(II)-loaded CaM when the protein interacts with α-synuclein, a small essentially unfolded cytoplasmic protein [96,97]. Chemical shift perturbation analysis indicates that the N-terminal part of α-synuclein interacts with both CaM domains. Rdc data were again collected for the C-terminal amide protons of CaM when

the latter has a terbium(III), thulium(III) or dysprosium(III) ion in the place of the calcium(II) ion in the second binding site, and the values were largely reduced with respect to those expected according to the tensors calculated from the pcs of the N-terminal domain. Such measurements thus indicated that the interaction with α-synuclein is highly fluxional, involving extensive motion of the two CaM domains. However, the spreading of the measured rdc data covers a range somewhat larger than observed for free CaM, as a consequence of a smaller conformational heterogeneity of the protein in the adduct. A larger range of the rdc data for the CaM C-terminal domain with respect to the free form has been also recently observed for the CaM complex with the CaM binding domain of Munc13-1 [98].

The conformation with largest MAP value obtained for CaM when bound to α-synuclein is not far from the "canonical" closed conformation of CaM. Other conformations with different interdomain orientations which have equally large rdc-derived MAP(R) values exhibit a relatively smaller MAP value, thus indicating that pcs are in this case effective in selecting and ranking the conformations according to the maximum allowed weight. In conclusion, in its complex with α-synuclein, CaM can experience multiple conformations, those with largest MAP being in a region of space close to that occupied by the canonical closed conformation. The weight of such conformation cannot however be larger than 0.35 [90].

The MAP approach can be also conveniently applied to study conformational heterogeneity in protein–protein adducts. Mobility in protein complexes has been recently investigated using SAXS and NMR data by analysing, besides pcs, the paramagnetic enhancement to the longitudinal relaxation rates [99]. The latter in fact scales as r^{-6}, where r is the nucleus–metal distance, according to Eq. (4) [100],

$$R_{1para} = \frac{k_1}{r^6}, \quad R_{2para} = \frac{k_2}{r^6} \tag{4}$$

where k_1 and k_2 are constants that depend on the nature of the metal ion and its electron relaxation time [101], on the nature of the observed nucleus, and on the reorientational time of the system. Paramagnetic spin labels were attached in different points of the protein cytochome *c* peroxidase [102], and the attenuation in the intensity in the signals of the partner protein iso-1-cytochome *c* due to paramagnetic broadening was used to delineate the conformational space sampled by the molecules.

Paramagnetic relaxation enhancements were analogously used to detect low population transient conformations under equilibrium conditions of a protein–DNA complex [103], and the presence of a minor form of the apo maltose-binding protein [104]. Paramagnetic relaxation enhancements can in fact be used to probe and structurally characterize the lowly populated regions of the free energy landscape through the analysis of the footprint of the minor conformations on the experimental data. This approach is possible when there is a rapid interconversion between the major and the minor conformations, so that the experimental relaxation rate enhancements increase with respect to the value corresponding to the major states in the presence of minor states with a sizably shorter distance between the paramagnetic center and the observed nuclei. Because of the sixth power dependence of the distance between the nucleus and the paramagnetic center (see Eq. (4)), the paramagnetic relaxation enhancement is very large at short distances, and therefore even lowly sampled conformations in which the nucleus is close to the paramagnetic center can be detected. Structural information can then be retrieved from multiple paramagnetic relaxation enhancements observed for a large number of protons from the discrepancies of the data that are not consistent with a single conformation of the system. In the case of the apo maltose-binding protein, the structure of the obtained minor form is similar to that calculated for the ligand-bound form, so that the predominant protein conformation coexists in a rapid equilibrium with the minor form, possibly facilitating the transition to the bound state [104].

Similarly to scoring all sterically allowed protein conformations according to their maximum occurrence, that has been proposed through the MAP/MO approach [90,95] previously described, spin labels were used to determine whether regions in the conformational space must be occupied or cannot be occupied by protein complexes by mapping out nuclei subject to paramagnetic relaxation enhancements, and thus coming close to the spin labels, and those showing no effects, and thus farther from them [102]. The available crystal structure for the complex of cytochrome *c* peroxidase and iso-1-cytochrome *c* represents the dominant protein–protein orientation also in solution, but ≈30% of the lifetime of the complex is spent in a dynamic encounter state. The observed paramagnetic effects were used to delineate the conformational space sampled by the protein molecules during the dynamic part of the interaction. A wide surface corresponding to the area that cannot be occupied by the center of mass of iso-1-cytochrome *c* for longer than 3% of the lifetime of the complex was so calculated, as well as the region which must contain the center of mass of iso-1-cytochrome *c* for at least 3% of the lifetime. After introduction of paramagnetic spin labels in 10 positions in cytochrome *c* peroxidase, and measurement of the corresponding relaxation enhancements in iso-1-cytochrome *c*, it was possible to sample the occurrence of interactions of the latter protein all around the entire surface of the former [105]. The averaged experimental data were found in agreement with a combination of 70% occurrence of the crystal conformation and 30% occurrence of an ensemble of conformations calculated with rigid-body Monte Carlo simulations in which only electrostatic and steric interactions were active. Such states correspond to a sampling of about 15% of the surface area of cytochrome *c* peroxidase, surrounding the binding interface observed in the crystal structure.

In another case, the conformational freedom within the complex between the proteins adrenodoxin and cytochrome *c* was investigated by determining the minimum degree of mobility of the system necessary to recover an agreement with the very small experimental pcs observed for adrenodoxin nuclei [99] when the two proteins are free in solution. Reduction in the pcs values with respect to those measured for the cross-linked proteins was in fact ascribed to interprotein dynamics. It was found that cyctochrome *c* needs to sample a large area on adrenodoxin. This result was confirmed by the small rdc values measured for adrenodoxin when a lanthanide tag is attached to cyctochrome *c* [40].

All these approaches, as well as the MAP or MO approach, are characterized by the search for the minimum or maximum lifetime that specific conformations or conformations within regions of the conformational space can have to be consistent with the available averaged experimental data. The latter cannot in fact provide the actual conformational ensemble as a unique solution.

2.4. Exploiting paramagnetism-based restraints for structural studies in solution

Besides being used to extract information on the conformational heterogeneity of proteins, pcs and rdc can be used, as reported since 1996 [106] and 1998 [107], respectively, to refine protein structures or protein domains assumed to be rigid. Pcs and rdc may in fact act as reporters of structural information because they depend on the position of the observed nuclei (for pcs) or on the orientation of the vector connecting dipole–dipole coupled nuclei (for rdc) with respect to the paramagnetic susceptibility anisotropy tensor (see Eqs. (1) and (2)) [28,108–111]. The structure of the N-terminal domain of CaM in the adduct with α-synuclein was, for example, calculated by including, among all distance and dihedral angle

✓ A paramagnetic metal ion is coordinated to one protein domain (A)
✓ Pcs and rdc are measured for both protein domains (A and B)

Case 1: The rdc span the same range of values in both protein domains ⇒ the two domains move rigidly

- the pcs of domain A provide the $\Delta\chi$ tensor
- the pcs and the rdc of domain A can be used to refine domain A. A new $\Delta\chi$ tensor can thus be estimated
- the pcs and the rdc of domain B can be used to locate such domain with respect to A and eventually to refine it, using the same $\Delta\chi$ tensor

Case 2: The rdc of domain A span a range of values much larger than those measured for domain B ⇒ there is interdomain mobility

- the pcs of domain A provide the $\Delta\chi$ tensor
- the pcs and the rdc of domain A can be used to refine domain A
- the rdc of domain B provide the $\Delta\tilde{\chi}$ tensor and can be used to refine domain B using such tensor
- pcs and rdc of domain B can be used to obtain information of the conformational ensemble

Scheme 1. Use of the paramagnetism-based restraints (pcs and rdc) for multidomain protein structure determination.

restraints, the pcs measured in the presence of the terbium(III), thulium(III) or dysprosium(III) ions substituted to the calcium(II) ion in the second metal binding site of the CaM domain [90]. On the contrary, the pcs measured for the C-terminal nuclei could not be used to calculate the structure of such domain because of its unknown mobility with respect to the N-terminal domain hosting the paramagnetic center. Differently from pcs, rdc measured for both the N-terminal and the C-terminal domain of CaM can be included in the structural calculation of the corresponding domain, provided that the appropriate anisotropy tensors are considered. For the N-terminal domain the tensors are the same as those calculated from the pcs collected on the same domain; for the C-terminal domain, the averaged tensors calculated from the averaged rdc data can be used (see Scheme 1).

Pcs and rdc are differently sensitive to local and global motions. Pcs are mostly sensitive to large global protein conformational changes, and are scarcely affected by local mobility and structural inaccuracies [29,80,90]. Rdc, on the other hand, are sensitive to even small local reorientations. These properties make it difficult to obtain a very accurate estimate of the magnetic susceptibility anisotropy tensor from rdc but, on the other hand, allow us to obtain a robust estimation of it through the pcs, once a structural model is available. Both pcs and rdc can then be used to refine the structure through such tensor (see Scheme 1). A new structural model is then calculated, and both tensor and structure can be refined iteratively. The independent availability of an accurate estimate of the orientation tensor from pcs actually permits a more quantitative use of rdc themselves for both structural and dynamical considerations.

Pcs and rdc have also been used for the accurate determination of protein solution structures starting from crystal structures. Crystal structures may in fact be inaccurate models of solution structures due to the presence of crystal packing forces. A possible strategy to improve the accuracy of a protein structure in solution is that of using a relatively good crystal structure as a starting model and refining it by applying well-selected, sensitive NMR restraints. Such approach was first applied through the use of pcs from a paramagnetic ion in a metalloprotein [112] and through the use of rdc originating from external orienting media in diamagnetic proteins [66,113]. Both pcs and rdc are long-range restraints and, therefore, optimally suited to detect global structural features, especially relative orientations of secondary structure elements or entire domains [35,66,80,90,114].

The combined use of the paramagnetism-based pcs and rdc for structural refinement starting from an X-ray structure was successfully demonstrated on CaM in its complex with two peptides representing the interaction sequence of two protein partners, the death-associated protein kinase (DAPk) and the DAPk-related protein 1 (DRP-1). New structural models were so calculated that are in excellent agreement with the paramagnetic restraints and differ modestly but significantly from the starting crystal structures. In these cases, the rdc measured for the C-terminal domain of CaM span ranges of values similar to those measured for the N-terminal domain, which contains the paramagnetic lanthanide. This indicates that in these complexes the two CaM domains have essentially a fixed conformation with respect to one another. The simultaneous use of pcs and rdc of the two CaM domains, and the knowledge that a unique magnetic anisotropy tensor for each metal ion is at the origin of all of them, pointed out the differences in the solution structure relative to the crystal structure. These differences consist of changes in the orientation of helix 1 in the first EF-hand of the N-terminal domain (this very same movement of helix 1 from the crystalline to the solution state was observed also by Bax et al. [66] in free CaM using rdc and external orienting media), and of the whole C-terminal domain, with respect to the metal-bearing second EF-hand of the N-terminal domain. The same approach can be used to reconstruct the structure of protein–protein complexes, once the structure of each protein is known. Again, SAXS/SANS data may be conveniently used together with the other restraints [94].

Therefore, the simultaneous use of paramagnetic pcs and rdc restraints may successfully: (i) indicate the possible presence of conformational freedom; (ii) provide an accurate estimate of the orientation tensor of the metal-bearing domain from pcs, which are less sensitive than rdc to the presence of local structural disorder or mobility; and (iii) provide the relative arrangement of proteins/domains/secondary structure elements with respect to the metal-bearing domain. Paramagnetic lanthanide labelling has been actually proposed as a fast NMR method to determine the structure of protein–protein complexes [35] as well as of protein–ligand complexes [115].

Pcs are also precious restraints for the structural determination of large proteins, for which it is still problematic to collect a large number of structural restraints [116]. Using three different attachment sites on the N-terminal domain of the protein STAT4, a homodimeric 29.4 kDa protein, for a cobalt(II) binding tag, long-range pcs were found distributed across the entire protein structure, thus enabling a much more accurate positioning of the protein secondary structural elements. Paramagnetic probes have been suggested also to disrupt the symmetry in the NMR spectra of

large protein homodimers such as the N-terminal domain of STAT4 [117]. These systems are in fact difficult to investigate because it is often hard to distinguish between intra and intermolecular NOEs. Sub-stoichiometric addition of a paramagnetic metal creates an asymmetric system, with the paramagnetic ion residing on only one subunit of the dimer. In this way, pcs and self-orientation rdc specific for each monomeric component of the symmetric dimer were obtained and used to properly position the subunits with respect to one another.

Recently, the solution structural model of the 65 kDa membrane-associated protein complex formed by adrenodoxin and adrenodoxin reductase was calculated through docking methods using as intermolecular restraints chemical shift perturbation data, pseudocontact shifts and paramagnetic relaxation enhancements arising from application of a paramagnetic tag in two positions, thus proving that sufficient restraints are provided by paramagnetism to determine the structural model of a protein complex in the case of low solubility and availability [118]. Starting from the structures of the isolated domains, rdc and paramagnetic relaxation enhancements have also be used for defining the structure of complexes. A general protocol is proposed consisting of (i) an initial refinement of the individual crystal structures to be in full agreement with observed rdc data and backbone dihedral angles, (ii) randomization of undefined protein regions and the relative orientation of the proteins, (iii) application of distance restraints from paramagnetic relaxation enhancements, (iv) structure calculation using rdc and relaxation enhancement data [119].

3. Exploiting paramagnetic restraints in solid-state structural studies

Solid-state NMR (SS-NMR) is a more and more attractive technique which is especially suited for membrane and insoluble proteins, fibrils, and proteins that do not crystallize properly. A major limitation of SS-NMR is however represented by the paucity of meaningful structural restraints [120–123]. Distance restraints can be obtained through experiments like proton-driven spin diffusion (PDSD) [121,124,124], CHHC [125], proton assisted recoupling (PAR) [126] and dipolar-assisted rotational resonance (DARR) [127]. A large part of the information, however, can be hardly recovered from the spectra because spectroscopic crowding and ^{13}C peak linewidths in many cases only permit ambiguous assignments. On the other hand, for microcrystalline samples, the assignment of the solid-state spectra can take advantage from the solution spectra assignment, because generally the ^{13}C chemical shifts do not change much on passing from solution to the microcrystalline state [11]. Protein–protein complexes or large protein aggregates may thus be conveniently investigated by SS-NMR thanks to the lack of line broadening due to the increase in molecular weight which is on the contrary observed with solution NMR.

In solid-state NMR, a source of line-broadening of NMR lines often operative for paramagnetic molecules in solution, Curie relaxation [128], is largely suppressed [129]. This makes the observation of NMR signals of paramagnetic metalloproteins little affected by paramagnetic relaxation, so that most of the signals arising from nuclei close to the paramagnetic center can be detected with standard solid-state NMR experiments [130]. A great advantage of a paramagnetic system is that many additional structural restraints become available after comparison of the NMR spectra with those of a diamagnetic analog, i.e. the pseudocontact shifts. Pcs suffer much less from the problem of ambiguity because they are directly obtained from the comparison of the assigned cross-peaks in the spectra used for sequential assignment of the paramagnetic and diamagnetic forms.

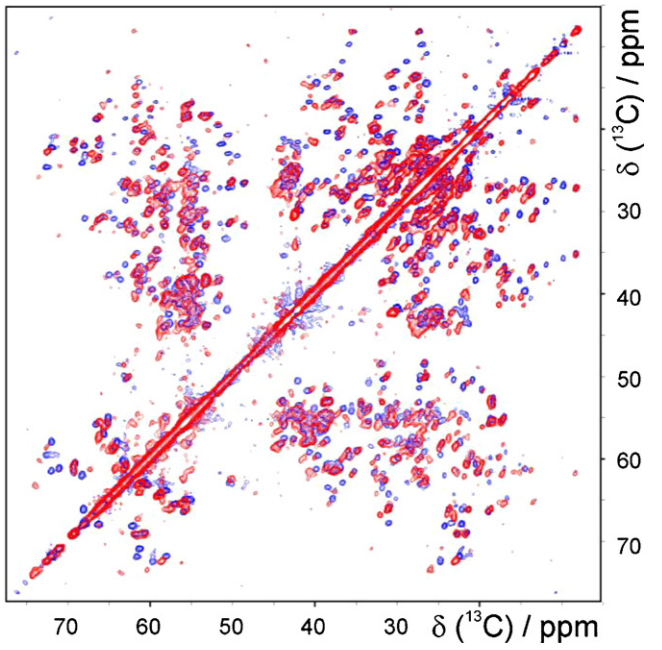

Fig. 5. Superimposition of the PDSD spectra (at 11.5 kHz MAS and 16.4 T) of diamagnetic ZnMMP-12 (blue contours) and of its paramagnetic CoMMP-12 (red contours) derivative.

The advantages provided by the availability of these restraints have been shown for the catalytic domain of MMP-12 (molecular mass 17.6 kDa). This protein contains a zinc(II) ion that can be substituted with a high-spin cobalt(II) ion [131]. The CP-MAS PDSD [124] spectra of both ZnMMP-12 and CoMMP-12 are of excellent quality (Fig. 5), and an almost complete assignment can be achieved [11]. From the superposition of the diamagnetic and paramagnetic spectra the presence of significant pcs for many ^{13}C signals is evident [132], and found in agreement with pcs measured for the same protein in solution. Therefore, as done in solution, pcs were used as restraints to determine the protein structure together with the other available restraints. However, it was soon realized that a small number of pcs have significant deviations from the values expected using Eq. (1), the available protein structure, and the magnetic susceptibility anisotropy tensor calculated from the other pcs. This is due to the fact that, in the solid state, metal ions within nearby protein molecules also contribute to the observed pcs (see Fig. 6), so that the experimental value for each nucleus is the sum of the contribution arising from the metal ion within the molecule (intramolecular pcs) and the contributions arising from all other metal ions in nearby molecules (intermolecular pcs) [132]. These contributions can be separated and used to provide different kinds of information. In fact, whereas intramolecular pcs constitute precious restraints for the calculation of the protein structure, intermolecular pcs can be used to obtain the relative arrangement of the protein molecules in the solid state. Intermolecular pcs may actually provide the position of the metal ions located in neighbouring molecules, and the orientation of the main axes of the magnetic susceptibility anisotropy tensor of the latter. This information was sufficient to locate and orient two nearby molecules, once the structure of the protein is known together with its magnetic susceptibility anisotropy tensor, determined by the intramolecular pcs [133].

Intramolecular and intermolecular pcs can be separated using two different combinations of protein labeling and dilution of the paramagnetic species [133]. A first sample was obtained using ^{13}C,^{15}N CoMMP-12 diluted with unlabeled ZnMMP-12, so that each labelled paramagnetic protein molecule is surrounded by diamag-

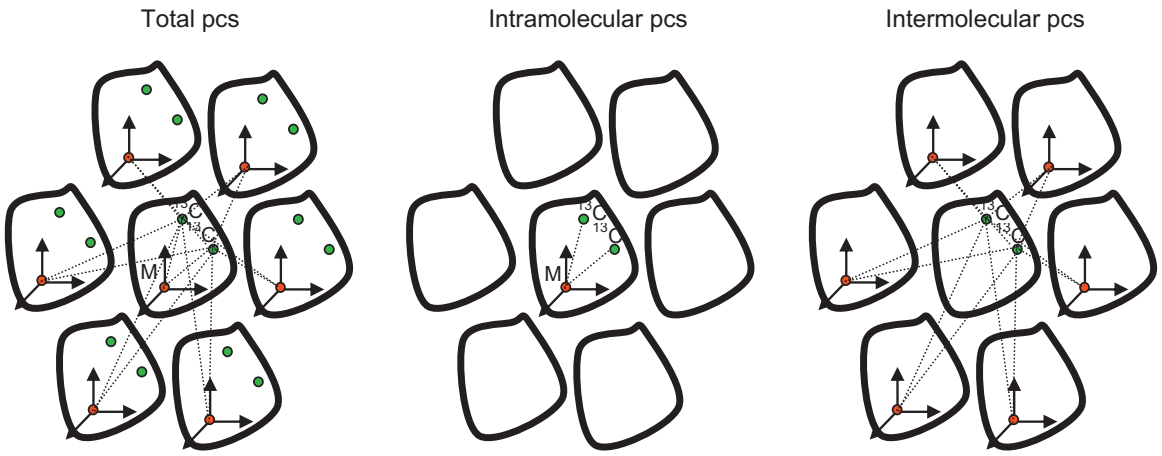

Fig. 6. The total pcs observed for a ^{13}C nucleus is given by the sum of the intramolecular contribution and intermolecular contributions. The former can be obtained by selective labelling of the molecules containing the paramagnetic metal diluted among unlabeled molecules; the latter by selective labelling of the molecules without the paramagnetic metal diluted among unlabeled molecules containing the paramagnetic metal ion.

netic molecules, and purely intramolecular pcs can be measured; a second sample was prepared using ^{13}C,^{15}N ZnMMP-12 diluted with unlabeled CoMMP-12, so that intramolecular pcs are absent (because only the nuclei in the labelled sample are observed) and purely intermolecular pcs can be measured (Fig. 6).

The intramolecular pcs (318 values) so measured were used to obtain the protein structure in the solid state with inclusion of other distance restraints from PDSD and CHHC spectra (284 values) and 153 angle restraints obtained from TALOS [134] prediction (Fig. 7). The improvement in the initial calculated structure upon addition of the pcs is remarkable, the backbone rmsd within the family decreasing from 5.8 to 3.0 Å. This means that the structure passes from being largely undefined to be folded in a reasonably good way. The availability of such structure provided information to solve a large number of ambiguities in the PDSD/DARR, CHHC, PAR [126] and PAIN-CP [135] spectra, extending the assignment of the latter and providing additional distance restraints in an iterative procedure. In this way, a total of 777 unambiguous distance restraints could be recovered, which, together with the pcs restraints, generated a more refined structural family (2KRJ) with backbone rmsd of 1.0 Å [136]. The rmsd between the mean of this family and the crystallographic X-ray structure (1RMZ) is 1.3 Å.

These results show that it may be convenient to use pcs as structural restraints in the solid state whenever it is possible to have a paramagnetic metal within the system under investigation, i.e. by attaching a paramagnetic metal binding tag [137] or expressing a metal-binding peptide in fusion with the investigated system [32]. Also intermolecular pcs may represent a valuable source of information in all cases when it is important to determine the relative arrangement of protein molecules, like for instance in fibril samples.

4. ^{13}C direct detection for paramagnetic systems in liquid and solid-state NMR

Paramagnetic metal ions are generally at the center of a "blind" sphere in which the NMR signals are too broad to be detected, due to the paramagnetic enhancement of the nuclear relaxation rates (see Fig. 8). The size of this sphere depends on the nature of the metal ion, on its electron relaxation rate, and on the gyromagnetic ratio γ of the detected nucleus [31,108]. Since the paramagnetic dipolar contribution to nuclear relaxation scales as γ^2, the radius of the blind sphere decreases of a factor $16^{1/6} \approx 1.6$ for ^{13}C nuclei with respect to ^{1}H nuclei, thus making ^{13}C direct detection NMR spectroscopy advantageous for the identification of nuclei in the proximity of the paramagnetic center and for the availability of structural restraints for these nuclei. A set of sequences enabling the complete assignment of proteins using ^{13}C direct detection has been developed [138–140]. It was shown that in the thulium-substituted derivative of calbindin D_{9k} the radius of the "blind"

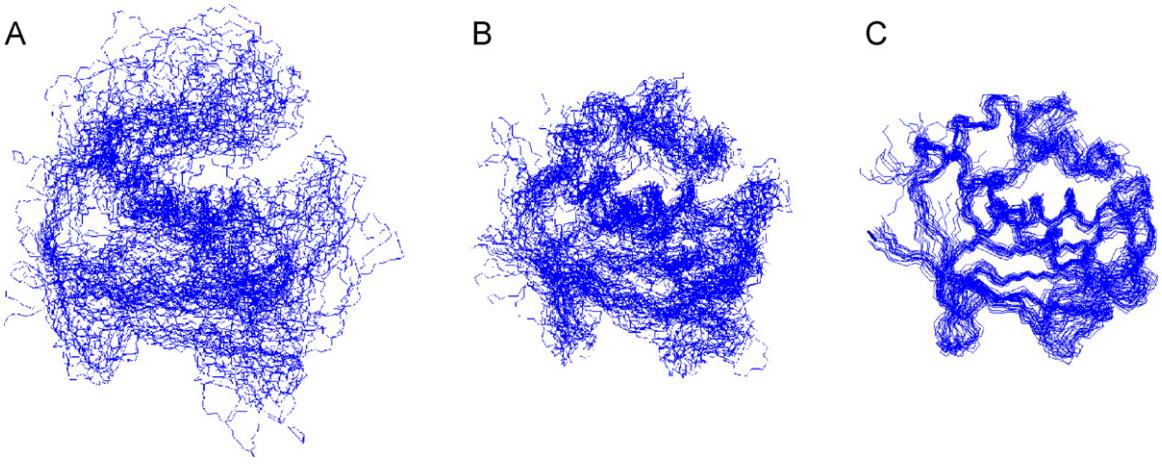

Fig. 7. Families of structures of MMP-12 obtained through SS-NMR (A) without paramagnetic restraints, (B) with paramagnetic restraints, and (C) with further addition of other distance restraints obtained by solving ambiguities in the PDSD/DARR, CHHC, PAR and PAIN-CP spectra thanks to the paramagnetic restraints.

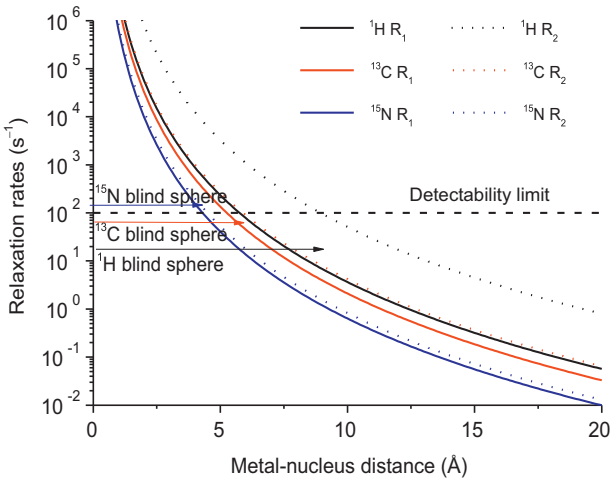

Fig. 8. Paramagnetic enhancement of the longitudinal and transverse relaxation rates as a function of the nuclear distance from the metal ion. The relaxation rates, and thus the line broadening, are higher for ^{1}H nuclei than for ^{13}C nuclei at the same distance from the metal, which in turn are higher than for ^{15}N nuclei. Calculations are performed assuming $S = 1/2$, a reorientational and an electron relaxation time of 2 ns, and a field corresponding to a proton Armor frequency of 700 MHz. The radius of the blind sphere for the different nuclei is set according to a detectability limit of 100 s^{-1}.

sphere decreases from 15 Å for ^{1}H signals to 9 Å for ^{13}C signals (and to 5 Å in ^{13}C 1D spectra) [141]. Similarly, in the monomeric form of copper-zinc superoxide dismutase (SOD), while ^{1}H signals within a sphere of 11 Å from the copper(II) ion are not detectable, all C' and C^{α} nuclei were assigned except those of the four copper(II) ligands, broadened beyond detection because of contact contributions to relaxation [142]. The paramagnetic enhancements to the nuclear relaxation rates were also used as restraints for the calculation of the protein solution structure, because they can be related to the metal-nucleus distances according to the Solomon equation (Eq. (4)) [29,100]. In this way the precision of the calculated structural family increased sizably, the backbone RMSD to the mean decreasing to 1.2 Å from the value of 1.6 Å obtained using only proton derived restraints, which had left some regions of the protein close to the metal ion very poorly defined [143]. Protocols for the measurement of rdc have also been developed through heteronuclear detection and proton-recoupled ^{13}C direct-detected experiments [144–146].

SS-NMR relies on homonuclear and heteronuclear experiments correlating ^{13}C and/or ^{15}N resonances of ^{13}C, ^{15}N labeled proteins. Progress in instrumentation and methodology has proceeded quite fast in the last years. Very nice spectra have been obtained for a microcrystalline sample of the paramagnetic oxidized SOD, clear enough to permit the identification of the ^{13}C spin system for each residue, including the histidine residues coordinating the copper(II) ion, so that nuclei as close as 5 Å from the metal could be detected [130]. Furthermore, methods for increasing resolution and sensitivity, through J-decoupling under MAS [147], or by selectively orienting polarization from the proton bath to a specific part of the carbon spectra more difficult to polarize [148], have been developed.

Magic angle spinning (MAS) in SS-NMR permits averaging of dipolar couplings of different strengths depending on the spinning frequency. High spinning frequency also provides gain in resolution and in the overall sensitivity, in particular for paramagnetic samples with short relaxation times [149]. Ultra-fast (60 kHz) MAS actually allows efficient detection in highly paramagnetic molecules: on the cobalt(II)-replaced catalytic domain of MMP-12, even the resonances from the residues coordinating the metal center, as close as 5.6 Å from the cobalt(II) ion, could be observed and assigned, opening the way to SS-NMR characterization of the metal coordination environment in metalloproteins. Furthermore, also pcs for nuclei as close as 6.2 Å to the metal, i.e. located in the metal binding loop and just before and after the coordinating histidines, could be measured [150].

5. Combining solution and solid-state NMR to study large molecules

In diamagnetic systems in solution, the NMR signal linewidth increases with the size of the macromolecule, so that proton based experiments can only provide partial information for systems larger than 100 kDa. On the other hand, the signal linewidth also depends on the magnitude of the nuclear magnetic moment of the observed nucleus (and of that of the dipole–dipole coupled nuclei). ^{13}C direct detection thus represents a valuable tool for studying large molecular systems, due to the smaller γ value of the ^{13}C nucleus with respect to the proton, as already seen in the previous section. An outstanding example of the synergy between ^{13}C detection in solution and in the solid state is represented by the NMR study of a 480 kDa protein, the multi-subunit ferritin

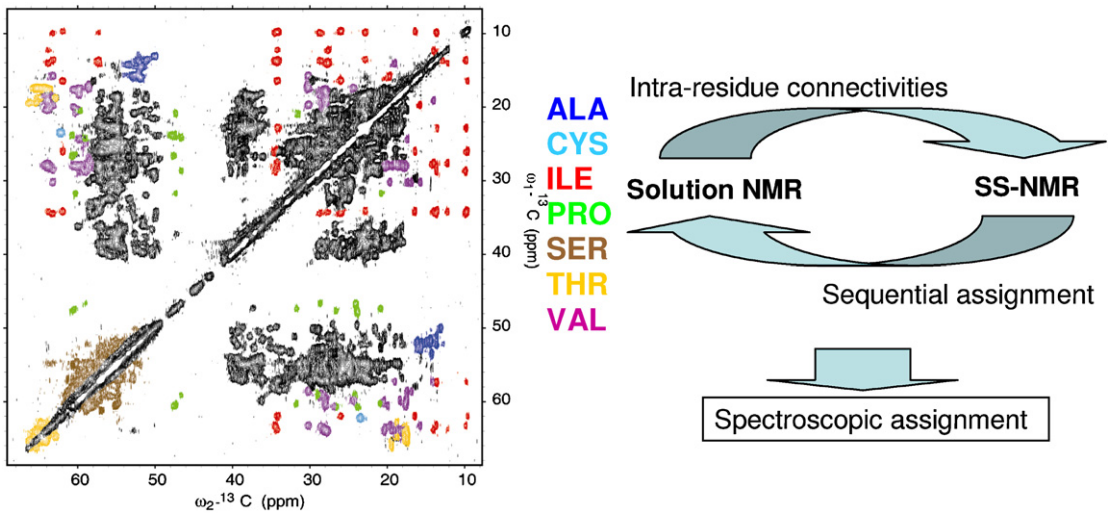

Fig. 9. ^{13}C–^{13}C NOESY spectrum of ferritin in solution. Some peaks are color-coded to exemplify the residue type assignment. The spectroscopic assignment of the protein is recovered by using intra-residue connectivities detectable in solution NMR spectra and the sequential assignment available from SS-NMR spectra.

nanocage. ^{13}C–^{13}C NOESY experiments performed on ferritin in solution allowed to detect intraresidue connectivities for most of the 174 residues of each subunit. The residue-specific chemical shifts of ^{13}C resonances then provided the spin patterns of most residues (Fig. 9), accounting for 75% of the total amino acids [151]. The rapid transverse relaxation induced by the slow molecular tumbling however prevented the use of the solution NMR experiments for the sequence-specific assignment. A partial sequence-specific assignment could be obtained through a unique approach including MAS SS-NMR experiments [152]. The solid-state PDSD and DARR spectra and the ^{13}C–^{13}C solution NOESY spectrum resulted in fact quite similar, providing the same kind of information, all with a relatively good resolution. The sequential assignment, obtained using solid-state 3D coherence transfer experiments [153] and transfer of assignments from solid-state spectra to the solution spectrum, of 59 residues distributed throughout each subunit was thus achieved. Paramagnetic broadening beyond detection of side chain signals in the ^{13}C–^{13}C solution NOESY spectrum induced by increasing concentrations of iron(III) species was then used to locate the iron(III) ions within each subunit, thus providing the identification of an iron channel for the transport from the active site toward the nanocage [152].

6. Concluding remarks

The need to investigate biological systems of larger and larger molecular weight as well as of characterizing their dynamics is nowadays a strong stimulus for advances in NMR. The large reorientation times of supramolecular protein complexes actually limit the applicability of solution NMR. Different methodologies have been developed to address the cases of large macromolecules, multi-domain proteins and protein–protein complexes. Paramagnetism-derived restraints proved quite efficient for determining the relative position of protein domains or of proteins within complexes. In conjunction with SAS data, both the structure and the conformational heterogeneity of the systems investigated can be addressed whenever they can be subdivided into small entities, the structure of which can be easily determined and assumed rigid. Structural information on the overall system is then recovered by determining the relative positions of these small entities using the information contained in pcs, rdc, paramagnetic relaxation enhancements and SAS profiles. This approach can be applied whatever the number of these entities is, up to the limiting case of unfolded proteins, where each residue should be considered separately.

TROSY-type techniques [154] permitted the successful application of solution NMR to protein systems up to 1 MDa [155,156]. Also MAS solid-state NMR represents a powerful tool for the investigation of large protein complexes and membrane proteins, once the system is conveniently crystallized or precipitated without crystal packing artefacts. Protein structures up to 17,600 Da have been solved through this technique [136]. Larger biological systems can be conveniently investigated taking advantage of both solid state and solution NMR in a synergistic way [152].

MAS solution NMR spectroscopy has been recently proposed for the study of large protein complexes in solution taking advantage of the MAS technique [157]. An efficient averaging of the anisotropic interactions, providing good spectroscopic resolution, was achieved by spinning the sample faster than the reorientation rate of the protein. The latter can be lowered by adjusting the protein concentration, temperature and viscosity of the solution. This approach has been proposed to be generally applicable to large protein complexes, with the advantages of overcoming protein size limitations of solution NMR without the need of sample crystallization/precipitation required by SS-NMR.

In conclusion, together with the development of more efficient methodologies and software needed to tackle the complexities of large biological systems, efforts are recommended for the development of optimized hardware and pulse sequences for SS-NMR as well as for the development of hardware and pulse sequences for heteronuclear detection, from which solution NMR of paramagnetic systems would largely take advantage. Finally, methods for sensitivity enhancements are needed for investigating systems which are difficult to obtain in large quantities like membrane proteins. An outstanding tool in this respect is provided by dynamic nuclear polarization (DNP). In the solid state, this technique largely enhances the NMR signal thanks to the transfer of electron spin polarization (usually related to a radical dissolved in the sample) to neighbouring nuclei [158–161]. Recently, extensive instrumentation advances have been made with the aim of applying the DNP mechanism also to biological systems in the liquid state, providing promising results [162–165].

Acknowledgements

This work has been supported by Ente Cassa di Risparmio, MIUR-FIRB contracts RBLA032ZM7, RBRN07BMCT and RBIP06LSS2, and by European Commission, contracts EU-NMR 026145, EAST NMR 228461 and SPINE2-COMPLEXES 031220.

References

[1] M.W.F. Fischer, L. Zeng, A. Majumdar, E.R.P. Zuiderweg, Proc. Natl. Acad. Sci. U.S.A. 95 (1998) 8016.
[2] R. Ishima, D.A. Torchia, Nat. Struct. Biol. 7 (2000) 740.
[3] F.A.A. Mulder, A. Mittermaier, B. Hon, F.W. Dahlquist, L.E. Kay, Nat. Struct. Biol. 8 (2001) 932.
[4] R. Brüschweiler, Curr. Opin. Struct. Biol. 13 (2003) 175.
[5] O.F. Lange, N.-A. Lakomek, C. Farès, G.F. Schröder, K.F.A. Walter, S. Becker, J. Meiler, H. Grubmüller, C. Griesinger, B.L. de Groot, Science 320 (2008) 1471.
[6] L.C. Wang, Y.X. Pang, T. Holder, J.R. Brender, A.V. Kurochkin, E.R.P. Zuiderweg, Proc. Natl. Acad. Sci. U.S.A. 98 (2001) 7684.
[7] E.Z. Eisenmesser, D.A. Bosco, M. Akke, D. Kern, Science 295 (2002) 1520.
[8] K. Lindorff-Larsen, R.B. Best, M.A. DePristo, C.M. Dobson, M. Vendruscolo, Nature 433 (2005) 128.
[9] Y.J. Huang, G.T. Montelione, Nature 438 (2005) 36.
[10] M. Fragai, C. Luchinat, G. Parigi, Acc. Chem. Res. 39 (2006) 909.
[11] S. Balayssac, I. Bertini, K. Falber, M. Fragai, S. Jehle, M. Lelli, C. Luchinat, H. Oschkinat, K.J. Yeo, ChemBioChem 8 (2007) 486.
[12] L.E. Kay, Nat. Struct. Biol. 5 (1998) 513.
[13] I. Bertini, Y.K. Gupta, C. Luchinat, G. Parigi, C. Schlörb, H. Schwalbe, Angew. Chem. Int. Ed. 44 (2005) 2223.
[14] C. Luchinat, G. Parigi, J. Am. Chem. Soc. 129 (2007) 1055.
[15] V. Borsi, C. Luchinat, G. Parigi, Biophys. J. 97 (2009) 1765.
[16] M. Akke, J. Liu, J. Cavanagh, H.P. Erickson, A.G. Palmer III, Nat. Struct. Biol. 5 (1998) 55.
[17] A.G. Palmer III, Chem. Rev. 104 (2004) 3623.
[18] E.R. Valentine, A.G. Palmer, Biochemistry 44 (2005) 3410.
[19] A. Mittermaier, L.E. Kay, Science 312 (2006) 224.
[20] I. Bertini, C.J. Carrano, C. Luchinat, M. Piccioli, L. Poggi, Biochemistry 41 (2002) 5104.
[21] J.R. Tolman, Curr. Opin. Struct. Biol. 11 (2001) 532.
[22] J.R. Tolman, J.M. Flanagan, M.A. Kennedy, J.H. Prestegard, Nat. Struct. Biol. 4 (1997) 292.
[23] J. Iwahara, C.D. Schwieters, G.M. Clore, J. Am. Chem. Soc. 126 (2004) 5879.
[24] G.M. Clore, C.D. Schwieters, J. Am. Chem. Soc. 126 (2004) 2923.
[25] G.M. Clore, C.D. Schwieters, J. Mol. Biol. 355 (2006) 879.
[26] J. Gsponer, H. Hopearuoho, S.B.-M. Whittaker, G.R. Spence, G.R. Moore, E. Paci, S.E. Radford, M. Vendruscolo, Proc. Natl. Acad. Sci. U.S.A. 103 (2006) 99.
[27] L. Nodet, L. Salmon, V. Ozenne, S. Meier, M.R. Jensen, M. Blackledge, J. Am. Chem. Soc. 131 (2009) 17908.
[28] I. Bertini, A. Donaire, B. Jiménez, C. Luchinat, G. Parigi, M. Piccioli, L. Poggi, J. Biomol. NMR 21 (2001) 85.
[29] I. Bertini, C. Luchinat, G. Parigi, Concepts Magn. Reson. 14 (2002) 259.
[30] L. Banci, I. Bertini, G. Cavallaro, A. Giachetti, C. Luchinat, G. Parigi, J. Biomol. NMR 28 (2004) 249.
[31] I. Bertini, C. Luchinat, G. Parigi, R. Pierattelli, Dalton Trans. 2008 (2008) 3782.
[32] J. Wöhnert, K.J. Franz, M. Nitz, B. Imperiali, H. Schwalbe, J. Am. Chem. Soc. 125 (2003) 13338.
[33] M. Prudêncio, J. Rohovec, J.A. Peters, E. Tocheva, M.J. Boulanger, M.E. Murphy, H.J. Hupkes, W. Koster, A. Impagliazzo, M. Ubbink, Chem. - Eur. J. 5 (2004) 3252.

[34] T. Ikegami, L. Verdier, P. Sakhaii, S. Grimme, P. Pescatore, K. Saxena, K.M. Fiebig, C. Griesinger, J. Biomol. NMR 29 (2004) 339.
[35] G. Pintacuda, A.Y. Park, M.A. Keniry, N.E. Dixonj, G. Otting, J. Am. Chem. Soc. 128 (2006) 3696.
[36] X.C. Su, T. Huber, N.E. Dixon, G. Otting, ChemBioChem 7 (2006) 1599.
[37] X.C. Su, B. Man, S. Beeren, H. Liang, S. Simonsen, C. Schmitz, T. Huber, B.A. Messerle, G. Otting, J. Am. Chem. Soc. 130 (2008) 10486.
[38] M.D. Vlasie, R. Fernández-Busnadiego, M. Prudêncio, M. Ubbink, J. Mol. Biol. 375 (2008) 1405.
[39] T. Zhuang, H.S. Lee, B. Imperiali, J.H. Prestegard, Protein Sci. 17 (2008) 1220.
[40] X. Xu, P.H.J. Keizers, W. Reinle, F. Hannemann, R. Bernhardt, M. Ubbink, J. Biomol. NMR 43 (2009) 247.
[41] P.H. Keizers, J.F. Desreux, M. Overhand, M. Ubbink, J. Am. Chem. Soc. 129 (2007) 9292.
[42] M.A.S. Hass, P.H.J. Keizers, A. Blok, Y. Hiruma, M. Ubbink, J. Am. Chem. Soc. 132 (2010) 9952.
[43] T. Saio, K. Ogura, M. Yokochi, Y. Kobashigawa, F. Inagaki, J. Biomol. NMR 44 (2009) 157.
[44] B. Man, X.C. Su, H. Liang, S. Simonsen, T. Huber, B.A. Messerle, G. Otting, Chem. Eur. J. 16 (2010) 3827.
[45] D. Häussinger, J. Huang, S. Grzesiek, J. Am. Chem. Soc. 131 (2009) 14761.
[46] X.C. Su, G. Otting, J. Biomol. NMR 46 (2010) 101.
[47] G. Pintacuda, M. John, X.C. Su, G. Otting, Acc. Chem. Res. 40 (2007) 206.
[48] K.N. Allen, B. Imperiali, Curr. Opin. Chem. Biol. 14 (2010) 247.
[49] I. Bertini, V. Calderone, M. Cosenza, M. Fragai, Y.-M. Lee, C. Luchinat, S. Mangani, B. Terni, P. Turano, Proc. Natl. Acad. Sci. U.S.A. 102 (2005) 5334.
[50] A. Page-McCaw, A.J. Ewald, Z. Werb, Nat. Rev. Mol. Cell Biol. 8 (2007) 221.
[51] J. Ottl, D. Gabriel, G. Murphy, V. Knauper, Y. Tominaga, H. Nagase, M. Kroger, H. Tschesche, W. Bode, L. Moroder, Chem. Biol. 7 (2000) 119.
[52] L.D. Chung, D. Dinakarpandian, N. Yoshida, J.L. Lauer-Fields, G.B. Fields, R. Visse, H. Nagase, EMBO J. 23 (2004) 3020.
[53] E.M. Tam, T.R. Moore, G.S. Butler, C.M. Overall, J. Biol. Chem. 279 (2004) 43336.
[54] D. Jozic, G. Bourenkov, N.H. Lim, R. Visse, H. Nagase, W. Bode, K. Maskos, J. Biol. Chem. 280 (2005) 9578.
[55] I. Bertini, V. Calderone, M. Fragai, R. Jaiswal, C. Luchinat, M. Melikian, E. Mylonas, D. Svergun, J. Am. Chem. Soc. 130 (2008) 7011.
[56] J.G. de la Torre, M.L. Huertas, B. Carrasco, J. Magn. Reson. 147 (2000) 138.
[57] D.I. Svergun, C. Barberato, M.H.J. Koch, J. Appl. Crystallogr. 28 (1995) 768.
[58] M.V. Petoukhov, D.I. Svergun, Biophys. J. 89 (2005) 1237.
[59] I. Bertini, M. Fragai, C. Luchinat, M. Melikian, E. Mylonas, N. Sarti, D. Svergun, J. Biol. Chem. 284 (2009) 12821.
[60] I. Bertini, M. Fragai, C. Luchinat, Curr. Pharm. Des. 15 (2009) 3592.
[61] G. Barbato, M. Ikura, L.E. Kay, R.W. Pastor, A. Bax, Biochemistry 31 (1992) 5269.
[62] J.L. Baber, A. Szabo, N. Tjandra, J. Am. Chem. Soc. 123 (2001) 3953.
[63] T. Wang, K.K. Frederick, T.I. Igumenova, A.J. Wand, E.R.P. Zuiderweg, J. Am. Chem. Soc. 127 (2005) 828.
[64] E. Carafoli, Proc. Natl. Acad. Sci. U.S.A. 99 (2002) 1115.
[65] R.R. Biekofsky, S.R. Martin, J.P. Browne, P.M. Bayley, J. Feeney, Biochemistry 37 (1998) 7617.
[66] J.J. Chou, S. Li, C.B. Klee, A. Bax, Nat. Struct. Biol. 8 (2001) 990.
[67] T. Yuan, H. Ouyang, H.J. Vogel, J. Biol. Chem. 274 (1999) 8411.
[68] E. Babini, I. Bertini, F. Capozzi, C. Luchinat, A. Quattrone, M. Turano, J. Proteome Res. 4 (2005) 1961.
[69] M.A. Wilson, A.T. Brunger, J. Mol. Biol. 301 (2000) 1237.
[70] C. Haynes, C.J. Oldfield, F. Ji, N. Klitgord, M.E. Cusick, P. Radivojac, V.N. Uversky, M. Vidal, L.M. Iakoucheva, PLoS. Comput. Biol. 2 (2006), e100–e100-12.
[71] J.D. Han, N. Bertin, T. Hao, D.S. Goldberg, G.F. Berriz, L.V. Zhang, D. Dupuy, A.J. Walhout, M.E. Cusick, F.P. Roth, et al., Nature 430 (2004) 88.
[72] M.R. Nelson, W.J. Chazin, Biometals 11 (1998) 297.
[73] S. Bhattacharya, C.G. Bunick, W.J. Chazin, Biochim. Biophys. Acta 1742 (2004) 69.
[74] S.-G. Chang, A. Szabo, N. Tjandra, J. Am. Chem. Soc. 125 (2003) 11379.
[75] W. Wriggers, E. Mehler, F. Pitici, H. Weinstein, K. Schulten, Biophys. J. 74 (1998) 1622.
[76] C.M. Shepherd, H.J. Vogel, Biophys. J. 87 (2004) 780.
[77] M.A. Schumacher, M. Crum, M.C. Miller, Structure 12 (2004) 849.
[78] J.L. Fallon, F.A. Quiocho, Structure 11 (2003) 1303.
[79] M. Zhang, T. Tanaka, M. Ikura, Nat. Struct. Biol. 2 (1995) 758.
[80] I. Bertini, C. Del Bianco, I. Gelis, N. Katsaros, C. Luchinat, G. Parigi, M. Peana, A. Provenzani, M.A. Zoroddu, Proc. Natl. Acad. Sci. U.S.A. 101 (2004) 6841.
[81] I. Bertini, I. Gelis, N. Katsaros, C. Luchinat, A. Provenzani, Biochemistry 42 (2003) 8011.
[82] X. Wang, S. Srisailam, A.A. Ye, A. Lemak, C. Arrowsmith, J.H. Prestegard, F. Tian, J. Biomol. NMR 39 (2007) 53.
[83] C. Eichmüller, N.R. Skrynnikov, J. Biomol. NMR 37 (2007) 79.
[84] J.R. Tolman, J.M. Flanagan, M.A. Kennedy, J.H. Prestegard, Proc. Natl. Acad. Sci. U.S.A. 92 (1995) 9279.
[85] I. Bertini, C. Luchinat, G. Parigi, Progr. NMR Spectrosc. 40 (2002) 249.
[86] I. Bertini, P. Kursula, C. Luchinat, G. Parigi, J. Vahokoski, M. Willmans, J. Yuan, J. Am. Chem. Soc. 131 (2009) 5134.
[87] A. Bax, N. Tjandra, Nat. Struct. Biol. 4 (1997) 254.
[88] A.A. Bothner-By, J.P. Domaille, C. Gayathri, J. Am. Chem. Soc. 103 (1981) 5602.
[89] M. Longinetti, C. Luchinat, G. Parigi, L. Sgheri, Inv. Probl. 22 (2006) 1485.
[90] I. Bertini, Y.K. Gupta, C. Luchinat, G. Parigi, M. Peana, L. Sgheri, J. Yuan, J. Am. Chem. Soc. 129 (2007) 12786.
[91] P. Bernadò, E. Mylonas, M.V. Petoukhov, M. Blackledge, D.I. Svergun, J. Am. Chem. Soc. 129 (2007) 5656.
[92] M.L. Mattinen, K. Paakkonen, T. Ikonen, J. Craven, T. Drakenberg, R. Serimaa, J. Waltho, A. Annila, Biophys. J. 83 (2002) 1177.
[93] P. Bernadò, L. Blanchard, P. Timmins, D. Marion, R.W.H. Ruigrok, M. Blackledge, Proc. Natl. Acad. Sci. U.S.A. 102 (2005) 17002.
[94] F. Gabel, B. Simon, M. Nilges, M.V. Petoukhov, D. Svergun, M. Sattler, J. Biomol. NMR 41 (2008) 199.
[95] I. Bertini, A. Giachetti, C. Luchinat, G. Parigi, M.V. Petoukhov, R. Pierattelli, E. Ravera, D.I. Svergun, J. Am. Chem. Soc 132 (2010) 13553.
[96] D. Lee, S.-Y. Lee, E.-N. Lee, C.-S. Chang, S.R. Paik, J. Neurochem. 82 (2002) 1007.
[97] J. Martinez, I. Moeller, H. Erdjument-Bromage, P. Tempst, B. Lauring, J. Biol. Chem. 278 (2003) 17379.
[98] F. Rodriguez-Castañeda, M. Maestre-Martinez, N. Coudevylle, K. Dimova, H. Junge, N. Lipstein, D. Lee, S. Becker, N. Brose, O. Jahn, et al., EMBO J. 29 (2010) 680.
[99] X. Xu, W. Reinle, F. Hannemann, P.V. Konarev, D.I. Svergun, R. Bernhardt, M. Ubbink, J. Am. Chem. Soc. 130 (2008) 6395.
[100] I. Solomon, Phys. Rev. 99 (1955) 559.
[101] I. Bertini, C. Luchinat, G. Parigi, Adv. Inorg. Chem. 57 (2005) 105.
[102] A.N. Volkov, J.A.R. Worrall, E. Holtzmann, M. Ubbink, Proc. Natl. Acad. Sci. U.S.A. 103 (2006) 18945.
[103] J. Iwahara, G.M. Clore, Nature 440 (2006) 1227.
[104] C. Tang, C.D. Schwieters, G.M. Clore, Nature 449 (2007) 1078.
[105] Q. Bashir, A.N. Volkov, G.M. Ullmann, M. Ubbink, J. Am. Chem. Soc. 132 (2010) 241.
[106] L. Banci, I. Bertini, K.L. Bren, M.A. Cremonini, H.B. Gray, C. Luchinat, P. Turano, J. Biol. Inorg. Chem. 1 (1996) 117.
[107] L. Banci, I. Bertini, J.G. Huber, C. Luchinat, A. Rosato, J. Am. Chem. Soc. 120 (1998) 12903.
[108] I. Bertini, C. Luchinat, G. Parigi, R. Pierattelli, ChemBioChem 6 (2005) 1536.
[109] I. Bertini, J. Faraone-Mennella, B.H. Gray, C. Luchinat, G. Parigi, J.R. Winkler, J. Biol. Inorg. Chem. 9 (2004) 224.
[110] R. Barbieri, C. Luchinat, G. Parigi, ChemPhysChem 21 (2004) 797.
[111] I. Bertini, Y.-M. Lee, C. Luchinat, M. Piccioli, L. Poggi, ChemBioChem 2 (2001) 550.
[112] M. Gochin, H. Roder, Protein Sci. 4 (1995) 296.
[113] N.R. Skrynnikov, N.K. Goto, D. Yang, W.-Y. Choy, J.R. Tolman, G.A. Mueller, L.E. Kay, J. Mol. Biol. 295 (2000) 1265.
[114] B.A. Fowler, F. Tian, H.M. Al-Hashimi, J.H. Prestegard, J. Mol. Biol. 304 (2000) 447.
[115] M. John, G. Pintacuda, A.Y. Park, N.E. Dixon, G. Otting, J. Am. Chem. Soc. 128 (2006) 12910.
[116] V. Gaponenko, S.P. Sarma, A.S. Altieri, D.A. Horita, J. Li, R.A. Byrd, J. Biomol. NMR 28 (2004) 205.
[117] V. Gaponenko, A.S. Altieri, J. Li, R.A. Byrd, J. Biomol. NMR 24 (2002) 143.
[118] P.H.J. Keizers, B. Mersinli, W. Reinle, J. Donauer, Y. Hiruma, F. Hannemann, M. Overhand, R. Bernhardt, M. Ubbink, Biochemistry 49 (2010) 6846.
[119] B. Simon, T. Madl, C.D. Mackereth, M. Nilges, M. Sattler, Angew. Chem. Int. Ed. 49 (2010) 1967.
[120] C.P. Jaroniec, C.E. MacPhee, V.S. Bajaj, M.T. McMahon, C.M. Dobson, R.G. Griffin, Proc. Natl. Acad. Sci. U.S.A. 101 (2004) 711.
[121] F. Castellani, B.J. van Rossum, A. Diehl, K. Rehbein, H. Oschkinat, Biochemistry 42 (2003) 11476.
[122] A. Lange, S. Becker, K. Seidel, K. Giller, O. Pongs, M. Baldus, Angew. Chem. Int. Ed. 44 (2005) 2089.
[123] W.T. Franks, B.J. Wylie, H.L. Schmidt, A.J. Nieuwkoop, R.M. Mayrhofer, G.J. Shah, D.T. Graesser, C.M. Rienstra, Proc. Natl. Acad. Sci. U.S.A. 105 (2008) 4621.
[124] F. Castellani, B. van Rossum, A. Diehl, M. Schubert, K. Rehbein, H. Oschkinat, Nature 420 (2002) 98.
[125] A. Lange, K. Seidel, L. Verdier, S. Luca, M. Baldus, J. Am. Chem. Soc. 125 (2003) 12640.
[126] G. De Paëpe, J.R. Lewandowski, A. Loquet, A. Böckmann, R.G. Griffin, J. Chem. Phys. 129 (2008) 245101.
[127] K. Takegoshi, S. Nakamura, T. Terao, Chem. Phys. Lett. 344 (2001) 631.
[128] M. Gueron, J. Magn. Reson. 19 (1975) 58.
[129] G. Kervern, S. Steuernagel, F. Engelke, G. Pintacuda, L. Emsley, J. Am. Chem. Soc. 129 (2007) 14118.
[130] G. Pintacuda, N. Giraud, R. Pierattelli, A. Böckmann, I. Bertini, L. Emsley, Angew. Chem. Int. Ed. 46 (2007) 1079.
[131] I. Bertini, M. Fragai, Y.-M. Lee, C. Luchinat, B. Terni, Angew. Chem. Int. Ed. 43 (2004) 2254.
[132] S. Balayssac, I. Bertini, M. Lelli, C. Luchinat, M. Maletta, K.J. Yeo, J. Am. Chem. Soc. 129 (2007) 2218.
[133] S. Balayssac, I. Bertini, A. Bhaumik, M. Lelli, C. Luchinat, Proc. Natl. Acad. Sci. U.S.A. 105 (2008) 17284.
[134] G. Cornilescu, F. Delaglio, A. Bax, J. Biomol. NMR 13 (1999) 289.
[135] J.R. Lewandowski, G. De Paëpe, R.G. Griffin, J. Am. Chem. Soc. 129 (2007) 728.
[136] I. Bertini, A. Bhaumik, G. De Paëpe, R.G. Griffin, M. Lelli, J. Lewandowski, C. Luchinat, J. Am. Chem. Soc. 132 (2010) 1032.
[137] P.S. Nadaud, J.J. Helmus, S.L. Kall, C.P. Jaroniec, J. Am. Chem. Soc. 131 (2009) 8108.
[138] W. Bermel, I.C. Felli, M. Matzapetakis, R. Pierattelli, E.C. Theil, P. Turano, J. Magn. Reson. 188 (2007) 301.
[139] W. Bermel, I. Bertini, I.C. Felli, R. Kümmerle, R. Pierattelli, J. Magn. Reson. 178 (2006) 56.

[140] W. Bermel, I. Bertini, I.C. Felli, M. Piccioli, R. Pierattelli, Progr. NMR Spectrosc. 48 (2006) 25.
[141] S. Balayssac, B. Jiménez, M. Piccioli, J. Biomol. NMR 34 (2006) 63.
[142] W. Bermel, I. Bertini, I.C. Felli, R. Kümmerle, R. Pierattelli, J. Am. Chem. Soc. 125 (2003) 16423.
[143] I. Bertini, I.C. Felli, C. Luchinat, G. Parigi, R. Pierattelli, ChemBioChem 8 (2007) 1422.
[144] M. Ottiger, F. Delaglio, A. Bax, J. Magn. Reson. 131 (1998) 373.
[145] P. Permi, P.R. Rosevear, A. Annila, J. Biomol. NMR 17 (2000) 43.
[146] S. Balayssac, I. Bertini, C. Luchinat, G. Parigi, M. Piccioli, J. Am. Chem. Soc. 128 (2006) 15042.
[147] S. Laage, A. Lesage, L. Emsley, I. Bertini, I.C. Felli, R. Pierattelli, G. Pintacuda, J. Am. Chem. Soc. 131 (2009) 10816.
[148] S. Laage, A. Marchetti, J. Sein, R. Pierattelli, H.J. Sass, S. Grzesiek, A. Lesage, G. Pintacuda, L. Emsley, J. Am. Chem. Soc. 130 (2008) 17216.
[149] S. Laage, J. Sachleben, S. Steuernagel, R. Pierattelli, G. Pintacuda, L. Emsley, J. Magn. Reson. 196 (2008) 133.
[150] I. Bertini, L. Emsley, M. Lelli, C. Luchinat, J. Mao, G. Pintacuda, J. Am. Chem. Soc. 132 (2010) 5558.
[151] M. Matzapetakis, P. Turano, E.C. Theil, I. Bertini, J. Biomol. NMR 38 (2007) 237.
[152] P. Turano, D. Lalli, I.C. Felli, E.C. Theil, I. Bertini, Proc. Natl. Acad. Sci. U.S.A. 107 (2010) 545.
[153] Y. Li, D.A. Berthold, H.L. Frericks, R.B. Gennis, C.M. Rienstra, ChemBioChem 8 (2007) 434.
[154] K. Pervushin, R. Riek, G. Wider, K. Wüthrich, Proc. Natl. Acad. Sci. U.S.A. 94 (1997) 12366.
[155] J. Flaux, E.B. Bertelsen, A.L. Horwich, K. Wüthrich, Nature 418 (2002) 207.
[156] R. Sprangers, L.E. Kay, Nature 445 (2007) 618.
[157] A. Mainz, S. Jehle, B.J. van Rossum, H. Oschkinat, B. Reif, J. Am. Chem. Soc. 131 (2009) 15968.
[158] D.A. Hall, D.C. Maus, G.J. Gerfen, S.J. Inati, L.R. Becerra, F.W. Dahlquist, R.G. Griffin, Science 276 (1997) 930.
[159] J.-H. Ardenkjaer-Larsen, B. Fridlund, A. Gram, L. Hansson, M.H. Lerche, R. Servin, M. Thaning, K. Golman, Proc. Natl. Acad. Sci. U.S.A. 100 (2003) 10158.
[160] C.-G. Joo, K.-N. Hu, J.A. Bryant, R.G. Griffin, J. Am. Chem. Soc. 128 (2006) 9428.
[161] V.S. Bajaj, M.L. Mak-Jurkauskas, M. Belenky, J. Herzfeld, R.G. Griffin, Proc. Natl. Acad. Sci. U.S.A. 106 (2009) 9244.
[162] T. Maly, G.T. Debelouchina, V.S. Bajaj, K.-N. Hu, C.-G. Joo, M.L. Mak-Jurkauskas, J.R. Sirigiri, P.C.A. Van der Wel, J. Herzfeld, R.J. Temkin, et al., J. Chem. Phys. 128 (2008) 052211.
[163] P. Höfer, G. Parigi, C. Luchinat, P. Carl, G. Guthausen, M. Reese, T. Carlomagno, C. Griesinger, M. Bennati, J. Am. Chem. Soc. 130 (2008) 3254.
[164] M.J. Prandolini, V.P. Denysenkov, M. Gafurov, B. Endeward, T.F. Prisner, J. Am. Chem. Soc. 131 (2009) 6090.
[165] M. Reese, M.-T. Tuerke, I. Tkach, G. Parigi, C. Luchinat, T. Marquardsen, A. Tavernier, P. Höfer, F. Engelke, C. Griesinger, et al., J. Am. Chem. Soc. 131 (2009) 15086.